

## **MODELLING OF THE FOOT TO IMPROVE SEGMENT POWER ESTIMATES**

**BIOMECHANICAL MODELLING OF THE FOOT  
TO IMPROVE SEGMENT POWER ESTIMATES  
IN THE VERTICAL JUMP**

by

**WENDY L. CARMICHAEL, B.Sc. / B.P.H.E.**

**A Thesis**

**Submitted to the School of Graduate Studies**

**in Partial Fulfilment of the Requirements**

**for the Degree**

**Master of Science**

**McMaster University**

© Copyright by Wendy L. Carmichael, September 1995.

**MASTER OF SCIENCE (1995)**  
**(Biomechanics)**

**McMASTER UNIVERSITY**  
**Hamilton, Ontario**

**TITLE:           Biomechanical Modelling of the Foot to Improve Segment Power  
                  Estimates in the Vertical Jump**

**AUTHOR:       Wendy L. Carmichael, B.Sc./B.P.H.E.   (Queen's University)**

**SUPERVISOR:     Dr. James J. Dowling, Ph. D.**

**NUMBER OF PAGES: xi , 80**

## **Abstract**

The present study develops a foot model to improve segment power estimates in the vertical jump. Modifications to the traditional foot model included the addition of a forefoot segment to allow for power flow across the metatarsal-phalangeal joint, and a re-definition of the ankle joint position to decrease foot segment length variability. The foot model was evaluated by comparison of the total segment power (TSP) with the rate of change of energy (RCE) of the foot segment. Pearson's correlation coefficients and percent root mean square (%RMS) error were used to compare curves.

Power flow analysis was performed on a counter-movement jump (CMJ) and a squat jump (SQJ) for each of 8 male and 8 female subjects. Both a 4-Link and a 5-Link, sagittal plane, link-segment model were used to calculate the joint and muscle powers.

The combination of both modifications to the traditional foot model (i.e. 5-Link(ankle) model), resulted in dramatic improvements for the match between the TSP and RCE. When comparing the traditional model with the 5-Link(ankle) model for the CMJ, correlation coefficients improved from -0.46 to 0.92 for the male group and from -0.50 to 0.77 for the female group. The %RMS error decreased from 380.5% to 35.4% for the male group and from 466.9% to 71.6% for the female group. SQJ improvements were similar.

Ankle joint position re-definition succeeded in compensating for foot segment

length changes in most cases, and indicates that a single point can be located to act as a hinge joint between the foot and leg segments throughout the vertical jump motion. Improvements associated with the addition of a forefoot segment to the traditional link-segment model indicate that substantial power flow occurs through the metatarsal-phalangeal joint during vertical jump motions.

## **Acknowledgements**

I would like to take this opportunity to thank my advisor, Dr. Jim Dowling, for his guidance and support. I would like to express my appreciation to my committee members, Dr. Michael Pierrynowski, Dr. Cindy Riach and Dr. Gail Frost, for their valuable insight and suggestions. I would also like to thank Michael for the use of the Human Movement Laboratory for data collection. Appreciation also goes out to the McMaster Volleyball Teams for their participation.

Thanks to my fellow graduate students, you know who you are, whose support and humour made this experience full of great memories. I would also like to thank Roger for his patience, encouragement and love throughout. Finally, I would like to thank my parents, Dugald and Hilda, and my brother, Ian, for their support and confidence.

## Table of Contents

<b>Abstract</b> . . . . .	iii
<b>Acknowledgements</b> . . . . .	v
<b>Table of Contents</b> . . . . .	vi
<b>List of Figures</b> . . . . .	viii
<b>List of Tables</b> . . . . .	xi
<b>Chapter 1 Introduction</b> . . . . .	1
<b>Chapter 2 Review of Literature</b> . . . . .	4
<b>2.1 Traditional Link-Segment Modelling</b> . . . . .	4
<b>2.2 Segment Power Flow Analysis</b> . . . . .	5
<b>2.3 The Ankle Joint</b> . . . . .	8
<b>2.4 Summary</b> . . . . .	9
<b>Chapter 3 Methods</b> . . . . .	10
<b>3.1 Subjects</b> . . . . .	10
<b>3.2 Experimental Protocol</b> . . . . .	10
<b>3.3 Data Collection</b> . . . . .	13
<b>3.4 Data Analysis</b> . . . . .	13
3.4.1 Data Reduction . . . . .	13
3.4.2 Segment Inertia Parameters . . . . .	14
3.4.3 Link-Segment Mechanics . . . . .	16
3.4.4 Total Segment Power Analysis . . . . .	16
3.4.5 Segment Rate of Change of Energy Analysis . . . . .	18
<b>3.5 Model Development</b> . . . . .	19
3.5.1 Addition of Forefoot Segment . . . . .	19
3.5.2 Modification of Ankle Joint Position . . . . .	21

<b>3.6</b>	<b>Statistical Measures</b>	21
3.6.1	Comparison of Models	21
3.6.2	Assessment of Foot Length Variability	22
<b>Chapter 4</b>	<b>Results</b>	<b>23</b>
<b>4.1</b>	<b>Foot Anthropometrics</b>	<b>23</b>
<b>4.2</b>	<b>Model Development</b>	<b>24</b>
4.2.1	Traditional 4-Link Model	25
4.2.2	Addition of Forefoot Segment	29
4.2.3	Ankle Location and its Effect on Foot Segment Length	32
4.2.4	Modificaton of Ankle Joint Position	35
4.2.5	Model Comparison	39
<b>4.3</b>	<b>Individual Subject Response to Model Modifications</b>	<b>41</b>
<b>4.4</b>	<b>Breakdown of TSP into JP and MP for Model Comparison</b>	<b>48</b>
4.4.1	Proximal Power Components (Ankle Joint)	48
4.4.2	Distal Power Components (M-p Joint)	49
<b>Chapter 5</b>	<b>Discussion</b>	<b>59</b>
<b>5.1</b>	<b>Model Development</b>	<b>59</b>
5.1.1	Addition of Forefoot Segment	60
5.1.2	Ankle Location and its Effect on Foot Segment Length	60
5.1.3	Modification of Ankle Joint Position	62
<b>5.2</b>	<b>Individual Subject Response to Model Modifications</b>	<b>63</b>
<b>5.3</b>	<b>Phases of Discrepancy (Comparionson with Walking)</b>	<b>64</b>
<b>Chapter 6</b>	<b>Conclusions</b>	<b>66</b>
<b>References</b>		<b>69</b>
<b>Appendix A</b>		<b>72</b>
<b>Appendix B</b>		<b>78</b>

## List of Figures

<b>Figure 1.</b>	IREM Marker Placement . . . . .	12
<b>Figure 2.</b>	Total Segment Power Calculations: 4-Link Model Foot versus 5-Link Model Foot . . . . .	20
<b>Figure 3.</b>	4-Link Model Total Segment Power (TSP) and Rate of Change of Energy (RCE) Curve Comparison for All Segments of a Typical Subject (M1) for a CMJ . . . . .	26
<b>Figure 4.</b>	4-Link Model Total Segment Power (TSP) and Rate of Change of Energy (RCE) Curve Comparison for All Segments of a Typical Subject (M1) for a SQJ . . . . .	27
<b>Figure 5.</b>	5-Link Model Total Segment Power (TSP) and Rate of Change of Energy (RCE) Curve Comparison for the Foot and Forefoot Segments of a Typical Subject (M1) for a CMJ and a SQJ . . . . .	30
<b>Figure 6.</b>	Comparison of Foot Length with Ankle Angle for a Typical Subject (M1) . . . . .	33
<b>Figure 7.</b>	Total Segment Power (TSP) and Rate of Change of Energy (RCE) Curve Comparison for the Foot Segment for a Typical Subject (M1) Under the Four Model Conditions for a CMJ . . . . .	36
<b>Figure 8.</b>	Total Segment Power (TSP) and Rate of Change of Energy (RCE) Curve Comparison for the Foot Segment for a Typical Subject (M1) Under the Four Model Conditions for a CMJ . . . . .	37
<b>Figure 9.</b>	Comparison of Foot Length with Ankle Angle for Subject F8 for a CMJ . . . . .	44

<b>Figure 10.</b>	Total Segment Power (TSP) and Rate of Change of Energy (RCE) Curve Comparison for the Foot Segment for a Subject F8 Under the Four Model Conditions for a CMJ . . . . .	45
<b>Figure 11.</b>	Comparison of Foot Length with Ankle Angle for Subject F5 for a CMJ . . . . .	46
<b>Figure 12.</b>	Total Segment Power (TSP) and Rate of Change of Energy (RCE) Curve Comparison for the Foot Segment for a Subject F5 Under the Four Model Conditions for a CMJ . . . . .	47
<b>Figure 13.</b>	Joint Power (JP) and Muscle Power (MP) Components of the Total Segment Power (TSP) for a Typical Subject (M1) Under the Four Model Conditions for a CMJ . . . . .	50
<b>Figure 14.</b>	Model Comparison of the Ankle Joint Power (JP) for a Typical Subject for a CMJ . . . . .	51
<b>Figure 15.</b>	Model Comparison of the Ankle Joint Reaction Forces and Ankle Velocities for a Typical Subject for a CMJ . . . . .	52
<b>Figure 16.</b>	Model Comparison of the Ankle Muscle Power (MP) for a Typical Subject for a CMJ . . . . .	53
<b>Figure 17.</b>	Model Comparison of the Ankle Moment and the Ankle Angular Velocity for a Typical Subject for a CMJ . . . . .	54
<b>Figure 18.</b>	Model Comparison of the M-p Joint Power (JP) for a Typical Subject for a CMJ . . . . .	55
<b>Figure 19.</b>	Model Comparison of the M-p Joint Reaction Forces and M-p Velocities for a Typical Subject for a CMJ . . . . .	56

**Figure 20.** Model Comparison of the M-p Muscle Power (MP)  
for a Typical Subject for a CMJ . . . . . 57

**Figure 21.** Model Comparison of the M-p Moment and  
the Ankle Angular Velocity for a Typical Subject  
for a CMJ . . . . . 58

## List of Tables

<b>Table 1.</b>	<b>Subject Characteristics</b> . . . . .	10
<b>Table 2.</b>	<b>Normative Anthropometric Values</b> . . . . .	15
<b>Table 3.</b>	<b>Measured Forefoot Parameters</b> . . . . .	23
<b>Table 4.</b>	<b>4-Link Model Correlation Coefficients for TSP and RCE</b> . . . . .	28
<b>Table 5.</b>	<b>4-Link Model %RMS Error for TSP and RCE</b> . . . . .	28
<b>Table 6.</b>	<b>5-Link Model Statistics for the Foot Segment</b> . . . . .	31
<b>Table 7.</b>	<b>5-Link Model Statistics for the Forefoot Segment</b> . . . . .	31
<b>Table 8.</b>	<b>Peak Forefoot Segment Power</b> . . . . .	32
<b>Table 9.</b>	<b>Correlation of Foot Length with Ankle Angle</b> . . . . .	32
<b>Table 10.</b>	<b>Ankle Marker Relocation Distance</b> . . . . .	34
<b>Table 11.</b>	<b>Segment Length Variability (Range/Mean * 100%)</b> . . . . .	34
<b>Table 12.</b>	<b>4-Link(ankle) Model Statistics for the Foot Segment</b> . . . . .	38
<b>Table 13.</b>	<b>5-Link(ankle) Model Statistics for the Foot Segment</b> . . . . .	39
<b>Table 14.</b>	<b>Correlation Coefficient Difference Scores for Model Comparison</b> . . . . .	40
<b>Table 15.</b>	<b>%RMS Difference Scores for Model Comparison</b> . . . . .	40
<b>Table 16.</b>	<b>Individual Statistics for the Foot Segment in all models for the CMJ</b> . . . . .	42
<b>Table 17.</b>	<b>Individual Statistics for the Foot Segment in all models for the SQJ</b> . . . . .	43

## **Chapter 1**

### **Introduction**

Vertical jump height is best predicted by the development of peak instantaneous positive power during the propulsive phase of the movement (Dowling & Vamos, 1993; Harman et al., 1990; Perrine et al., 1978). This power is calculated for the whole body as the product of the ground reaction force and the vertical velocity of the centre of gravity. In order to examine the development of that peak power, it would be useful to determine the flow of power which occurs within and between the segments contributing to the movement.

Segment power flow analysis is a method used to yield information about the generation, absorption and transfer of mechanical energy in human movements. This method distinguishes between the segment energy that is generated, absorbed or transferred actively by muscular contraction (muscle power), and that which is transferred passively via joint attachments from an adjacent segment (joint power). The ability to distinguish between these two sources will provide information about the function and importance of the active muscle groups to the vertical jump.

Joint power (JP) is calculated as the product of the joint reaction force and the linear velocity of the joint centre, while muscle power (MP) is calculated as the product of the net muscle moment and the angular velocity of the segment (Elftman, 1939a;

Quanbury et al., 1975; Robertson & Winter, 1980; Winter et al., 1976). In order to validate these measures of power, Robertson and Winter (1980) compared the total segment power of the thigh, leg and foot during walking to the segment rate of change of mechanical energy. Power measures were validated for all segments except the foot during the weight acceptance and the late push-off phase of the gait cycle. As a result, application of this method to the study of athletic movements thus far, has focused on motions where the foot is not in contact with the ground (Chapman & Caldwell, 1983; Vardaxis & Hoshizaki, 1989; Young & Martenuik, 1995). A valid foot model has yet to be developed for application to weight bearing activities.

Theoretically, for any rigid segment, the rate of change of energy (RCE) should be equal to the total segment power (TSP) calculated by the sum of the individual joint and muscle powers (van Ingen Schenau & Cavanagh, 1990). Differences between methods have been attributed to the limitations of traditional two-dimensional (2D) link-segment modelling as it pertains to the calculation of the joint and muscle powers (Robertson & Winter, 1980; Vardaxis & Hoshizaki, 1989; de Looze et al., 1992). More specifically, van Ingen Schenau and Cavanagh (1990, p. 872) have attributed the main cause of the errors in the calculation of total segment power to the "necessary assumptions concerning the rigidity of the links and the position of the (moving) axes of rotation."

For traditional 2D link-segment modelling, the foot is represented as a rigid triangle defined by the ankle joint, the metatarsal-phalangeal (m-p) joint and the heel.

The base of this triangle is where the ground reaction forces are applied to the system. The triangle does not extend to the great toe because of the plantarflexion and dorsiflexion which occur at the m-p joint (Winter, 1983). Excluding a forefoot segment neglects the potential for power to be generated by the m-p flexors and/or transferred at the m-p joint.

The purpose of the present study was to develop a foot model to improve segment power estimates in the vertical jump. In order to accomplish this goal, it was necessary to examine the effect of adding a forefoot segment to the traditional foot model and to determine a method to decrease the foot segment length variability.

## **Chapter 2**

### **Review of Literature**

#### **2.1 Traditional Link-Segment Modelling**

To investigate the internal forces that cause movement, researchers represent the human body as a series of rigid segments linked together by fixed hinge joints. The development of this link-segment model allows the application of classical mechanics to the human body. The assumptions made with respect to the model are summarized by Winter (1990, p.76) and are as follows:

1. Each segment has a fixed mass located as a point mass at its centre of mass.
2. The location of each segment's centre of mass remains fixed during the movement.
3. The joints are considered to be hinge (or ball and socket) joints.
4. The mass moment of inertia of each segment about its mass centre is constant during the movement.
5. The length of each segment remains constant during the movement.

The internal forces acting on each of these link-segments can be estimated using inverse dynamics. This method uses measured kinematic data, estimated anthropometric data and values of external forces to calculate the joint reaction forces and net muscle moments. The accuracy of the estimated forces and torques are dependant on accurate kinematic measures, good anthropometric estimates, accurately located joint centres of rotation, and good measures of external force.

Traditionally, the foot is modelled as a rigid triangle that is defined at each apex by the ankle joint, the m-p joint and the heel. The triangle does not extend to the great toe because of the plantarflexion and dorsiflexion which occur at the m-p joint (Winter, 1983). The ground reaction forces which are distributed over the area of the foot are represented as a single vector acting at a single point on the base of the foot known as the centre of pressure. The foot segment is usually defined simply as the line between the m-p and ankle marker.

## **2.2 Segment Power Flow Analysis**

In order to gain a better understanding of muscle function in human locomotion, Elftman (1939a,b) proposed methods to include the rate at which the muscles do work (power) on the foot, leg, thigh and trunk segments in his analysis of the dynamics of the human leg during walking. Using data from a force platform, he calculated joint reaction forces and moments of force about each joint. The rate at which energy is transferred due to joint reaction forces and the rate at which muscles do work on each leg segment was determined by combining these forces and moments with the velocities of their points of application. More recently, Quanbury, Winter and Reimer (1975) presented a more detailed and mathematical discussion of Elftman's work as well as a second method of calculating the instantaneous power of a body segment. This second method calculates the rate of change of the total energy of the segment as the time derivative of the sum of its potential, translational kinetic and rotational kinetic energies.

Theoretically, for any rigid segment, the rate of change of energy (RCE) should be equal to the total segment power (TSP) calculated from the sum of the individual joint and muscle powers (van Ingen Schenau & Cavanagh, 1990). The TSP is often compared with the RCE to validate the link-segment model used to calculate the joint and muscle powers (Robertson & Winter, 1980; Vardaxis & Hoshizaki, 1989; Young & Marteniuk, 1995). RCE is assumed to be more accurate than TSP because it is based on first derivative kinematics and anthropometric data only, whereas TSP is additionally based on second derivative kinematics, force platform data and locations of the joint centres of rotation (Robertson & Winter, 1980).

In practice, these two methods of calculation seem to be in very good agreement for the swing phase of walking ( $r \geq 0.989$  for foot, leg and thigh, Robertson & Winter, 1980; Quanbury et al., 1975), the recovery phase of sprinting ( $r \geq 0.98$  for foot, leg, and thigh, Vardaxis & Hoshizaki, 1989) and for all segments except the foot ( $r = 0.815$  to  $0.978$  for leg, thigh, Robertson & Winter, 1980) in the stance phase of walking. Poor agreement for the foot segment is especially evident during weight acceptance and the late push-off phase of the gait cycle ( $r = -0.489$  to  $0.390$ , Robertson & Winter, 1980). Discrepancies between methods have been attributed to experimental error and/or violation of the underlying assumptions of link-segment modelling.

In a survey article, van Ingen Schenau and Cavanagh (1990, p.872) have attributed the main cause of the errors in the calculation of TSP to the "necessary assumptions concerning the rigidity of the links and the position of the (moving) axes of

rotation." Robertson and Winter (1980) found through error analysis that the location of the ankle centre of rotation was influential on the TSP calculations but had little effect on the RCE. de Looze et al. (1992) have demonstrated the importance of a constant segment length to the calculation of TSP. More recently, Winter and Ishac (1994) have attributed poor agreement of the foot segment values during weight acceptance to energy absorption by the heel fat pad and shoe material. During push-off, discrepancies have been attributed to an energy absorption in the flexing m-p joint and flexing of the sole of the shoe followed by an energy burst from the m-p plantarflexors (Winter & Ishac, 1994). A forefoot segment in a link-segment model, incorporating m-p muscle power or transfer of power at the m-p joint, has yet to be included in this sort of analysis.

Application of segment power flow analysis thus far, has focused on athletic movements where the foot is off the ground. Studies have looked at the energy input into each lower limb segment during the swing phase in treadmill running (Chapman & Caldwell, 1983), the power patterns of advanced and intermediate sprinters during the recovery phase of a sprinting stride (Vardaxis & Hoshizaki, 1989), the acquisition of a multi-articular kicking task (Young & Marteniuk, 1995), and the work and energy transfer estimates in the recovery leg in walking and running (Caldwell & Forrester, 1992). Fukashiro and Komi (1987) have reported a joint moment and mechanical power flow analysis of the lower limb for a single subject during the vertical jump. Although the rate of change of mechanical energy is included in one figure, a comparison of the two methods of power calculation is notably absent from their discussion, and as a result, the validity of the reported joint and muscle powers is suspect.

### 2.3 The Ankle Joint

Two-dimensional link-segment modelling requires proper identification of the locations of hinge-joint articulations between adjoining segments. Of particular importance to the foot segment, is the precise location of an ankle joint. Motion between the foot and the leg segment results from the movements of two main joints that make up the ankle complex. These are the articulation between the tibia and the talus, referred to as the ankle joint, and the articulation between the talus and the calcaneus, referred to as the subtalar joint. Plantarflexion and dorsiflexion are usually attributed to the ankle joint, with inversion and eversion attributed to the subtalar joint (Clemente, 1985; Lehmkuhl & Smith, 1983).

It has been shown, however, that the range of motion in the sagittal plane between the foot and the leg segment is greater than the range of motion in the ankle joint alone (Siegler et al., 1988). Moreover, Siegler et al. (1988) found that the subtalar joint contributed about 20% of the total range of plantarflexion and dorsiflexion of the ankle complex, this contribution occurring primarily at the extremes of the range of motion. Their study was conducted on unweighted cadaver limbs and therefore can not be directly applied to subjects performing weight bearing activities (Siegler et al., 1988).

Inman (1976) identified the axis of rotation of the ankle joint as a line joining two points just distal to each malleolus. Despite reports suggesting that the ankle joint does not act as an ideal hinge joint with a fixed axis of rotation (Lundberg et al., 1989; Sammarco, 1977; Siegler et al., 1988), it is necessary to estimate a point where an ideal

articulation connects the leg and foot segments for 2D link-segment modelling. This point is typically landmarked as the most distal end of the lateral malleolus of the fibula. If this location is a poor estimate, foot segment length changes would be observed as the ankle dorsi- and plantar-flexed.

## **2.4 Summary**

From the above review of literature, it is evident that in order to perform a power flow analysis on weight bearing activities, it will be necessary to develop a foot model which will provide a good match between the TSP and RCE. Discrepancy between the TSP and RCE curves for the traditional foot model has been attributed to flexion and extension of the m-p joint during push-off. Although to date, a model with a forefoot segment has not been utilized. Discrepancy between the two curves could also be due to violations of the link-segment modelling assumptions associated with the calculation of the TSP. The link-segment model requires the identification of hinge joint locations, to act as links between the adjoining segments. Of particular importance to the foot segment is the location of the centre of rotation of the ankle joint. Poor estimation of the ankle joint location may be observed as changes in foot segment length throughout the jumping motion.

## Chapter 3

### Methods

#### 3.1 Subjects

Sixteen university or club volleyball players (8 male, 8 female) volunteered to participate in the study. Volleyball players were recruited because of the frequency of two-foot vertical jumps which occurs in this sport, and the common use of these athletes in jumping studies. Subject characteristics are listed in Table 1. All participants were given verbal and written instructions about the experimental protocol and signed an informed consent form.

**Table 1 Subject Characteristics**

Parameter	Males		Females	
	Mean	SD	Mean	SD
Age (yrs)	20.9	1.4	21.8	1.8
Height (cm)	186.2	8.2	174.4	5.7
Total Body Mass (kg)	83.6	13.1	66.9	6.2

SD = standard deviation; yrs = years

#### 3.2 Experimental Protocol

Measures of height and total body mass were recorded. Right forefoot length and width were measured with anatomical calipers. Forefoot length was measured from the

fifth metatarsal-phalangeal (m-p) joint to the end of the great toe, and forefoot width was measured from the first to the fifth m-p joint. The right foot of each subject was then immersed in a beaker of water to the level of the fifth metatarsal-phalangeal (m-p) joint. This procedure was performed three times and the mean value was used to represent that individual's forefoot volume.

Subjects were instructed to warm-up prior to testing. Infrared emitting diodes (IRED) markers were placed on the following landmarks on the right side of the body: toenail of the great toe, fifth m-p joint, distal tip of the lateral malleolus, posterior convexity of the femoral condyle, tip of the greater trochanter, and the glenohumeral joint. The end of the forefoot segment was determined via translation from the toe marker to the height of the m-p marker. The translation also compensated for dorsi/plantarflexion of the forefoot segment. Refer to Figure 1 for a schematic of marker placement.

Subjects were instructed to perform warm-up jumps to familiarize themselves with the constraints of taking-off and landing on the force platform. The required task consisted of three successful maximum-effort counter-movement jumps (CMJ) followed by three successful maximum-effort squat jumps (SQJ) on a force platform. All successful jumps began and ended on the force platform. Subjects were barefoot and were instructed to keep their hands on their hips for all jumps. An average minimum CMJ knee angle was determined for each subject for the three CMJ trials. Subjects were instructed to assume and hold this knee angle prior to performing the SQJ.

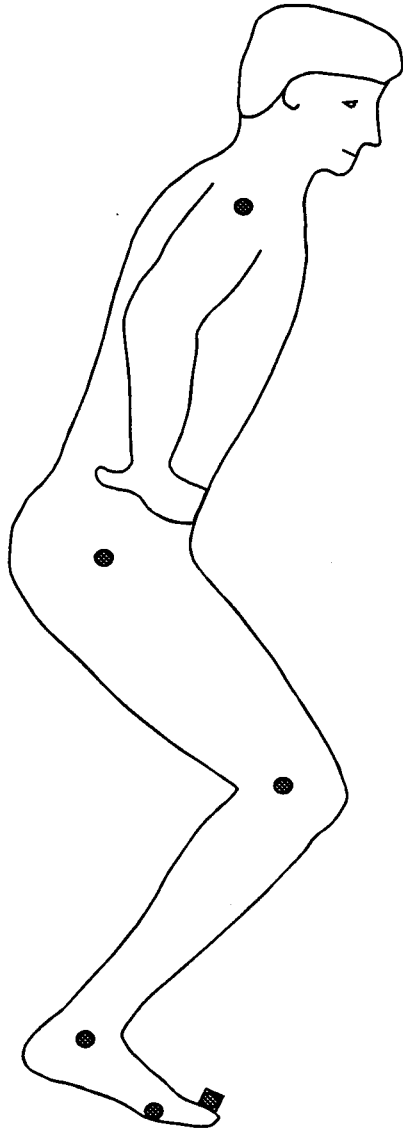


**Figure 1.** IRED Marker Placement

### **3.3 Data Collection**

Marker movements were sampled using an optoelectronic three-dimensional motion measurement system (OPTOTRAK/3020, Northern Digital, Inc., Waterloo, Canada). The camera unit was positioned horizontally and was placed at right angles to the subject's sagittal plane at a distance of 6 metres. Ground reaction forces and moments were registered through a multi-component force platform (AMTI model OR6-5, Advanced Mechanical Technology, Inc., Massachusetts, USA). Data were channelled to an OPTOTRAK Data Acquisition Unit (ODAU) for A/D conversion (12 bit) and to synchronize the kinematic and kinetic data. Kinematic and kinetic data were collected at 100Hz, using an IBM compatible, 486 based, 66MHz personal computer.

### **3.4 Data Analysis**

#### **3.4.1. Data Reduction**

All jumps were analyzed from the instant the force-time curve deviated from the body-weight line (initiation of jumping motion) until the force platform record indicated that takeoff had occurred. For each subject, one trial from each of the CMJ and SQJ types was chosen for further analysis. The selection criteria for the CMJ was based on the best performance of the three trials, measured as time in the air. The selection criteria for the SQJ was similar to that of the CMJ, however SQJ trials with any counter-movement were disqualified.

A two-dimensional, sagittal-plane, link-segment analysis was performed. The x-axis defined the horizontal direction and the y-axis defined the vertical direction, with

positive directions anteriorly and superiorly, respectively. Kinematic data processing software was developed to interpolate missing OPTOTRAK data points using cubic spline estimation. Marker positions were filtered using a dual-pass, critically-damped, low-pass filter with a cutoff frequency of 7Hz. This cutoff frequency was determined using residual analysis (Winter, 1990). Linear and angular velocities and accelerations were calculated by differentiation of displacement data using central finite differences. Kinetic data processing software was developed which used the AMTI calibration matrix to convert force platform data from millivolts to force and moments of force, and to calculate the centre of pressure in the x-direction.

#### 3.4.2. Segment Inertia Parameters

Segment mass, position of centre of mass, and radius of gyration were estimated for the HAT, thigh, leg and foot segments from values listed in Table 2. Forefoot mass was determined by multiplication of the forefoot volume with Dempster's (1955) specific density of the foot. Individual values of forefoot mass were expressed as a percentage of the total body mass. Group means were determined by averaging these values. Hindfoot mass was determined by subtracting the mean forefoot mass from the Table 2 values for the whole foot. The position of the centre of mass and the magnitude of the moment of inertia were determined by modelling the forefoot segment as a right triangular prism. Parameters for the hindfoot were calculated by subtracting the forefoot parameters from the foot parameters using composite body mechanics (see Appendix A).

**Table 2 Normative Anthropometric Values**

Segment	Definition	Segment Mass as % Total Body Mass		Centre of Mass / Segment Length (Proximal)		Radius of Gyration / Segment Length (Centre of Mass)	
		M	F	M	F	M	F
Forefoot (x2)	Head of metatarsal V/ Tip of great toe	0.48C	0.45C	0.333C	0.333C	0.252C	0.249C
Hindfoot (x2)	Tip of lateral malleolus of fibula / Head of metatarsal V	2.38CP	2.21CP	0.346CP	0.337CP	0.361CP	0.350CP
Foot (x2)	Tip of lateral malleolus of fibula / Head metatarsal V	2.86P	2.66P	0.500P	0.500P	0.475P	0.475P
Leg (x2)	Posterior convexity of lateral femoral condyle/ Tip of lateral malleolus of fibula	9.5P	10.7P	0.434P	0.419P	0.302CP	0.298CP
Thigh (x2)	Greater trochanter/ Posterior convexity of lateral femoral condyle	21.0P	23.5P	0.433P	0.428P	0.323CP	0.321CP
HAT	Greater trochanter/ Glenohumeral Joint	66.64CP	63.14CP	0.626W	0.626W*	0.496W	0.496W*

\* no female values were available for a HAT segment therefore male values were used.

Source Codes: P, Dempster via Plagenhoef et al. (1983) from living subjects; Anatomical Data for Analyzing Human Motion, *Research Quarterly for Exercise and Sport*, v. 54, no. 2, pp. 169-178. W, Dempster via Winter (1990); *Biomechanics and Motor Control of Human Movement*, John Wiley & Sons, New York. C, Calculated. CP, calculated from Plagenhoef et al. (1983).

### 3.4.3 Link-Segment Mechanics

A traditional two-dimensional link-segment model was used (Winter, 1990), which included either four or five segments. The four segment model included; the foot, shank, thigh, and HAT segments joined by the ankle, knee and hip joints. The five segment model included; the forefoot, foot, leg, thigh, and HAT segments joined by the metatarsal-phalangeal (m-p), ankle, knee and hip joints. Standard linked segment mechanics (Winter, 1990) were used to calculate joint reaction forces and muscle moments at each joint. Segment lengths were taken as the distance between the two defining end-point markers. The analysis began at the most distal segment where the ground reaction force and its point of application were known.

### 3.4.4. Total Segment Power Analysis

Total segment power was determined by first calculating the individual joint and muscle powers.

Each joint power (JP) was calculated using the following formula:

$$JP = R_x * v_x + R_y * v_y \quad (1)$$

where,  $R_x$  and  $R_y$  are the reaction force components acting on the segment.

$v_x$  and  $v_y$  are the linear velocity components of the segment end points.

Each muscle power (MP) was calculated using equation (2):

$$MP = M * \omega \quad (2)$$

where,  $M$  is the moment of force acting on the segment.  
 $\omega$  is the angular velocity of the segment.

The total segment power (TSP) of each segment was then calculated using equation (3):

$$TSP = [JP + MP]_{prox} + [JP + MP]_{dist} \quad (3)$$

where,  $[ ]_{prox}$  and  $[ ]_{dist}$  denote the proximal and distal ends of the segment.

It should be noted that the total segment power of the most distal segment is simply the sum of the proximal power terms. This occurs because there are no joint reaction forces or muscle moments associated with the free ends of a link-segment model. Similarly, the total segment power of the most proximal segment only has distal power terms.

### 3.4.5. Segment Rate of Change of Energy Analysis

The segment rate of change of energy was derived by first calculating the instantaneous mechanical energy of each segment ( $E_i$ ) as the sum of its potential, translational kinetic and rotational kinetic energies as follows:

$$E_i = mgh + \frac{1}{2}mv^2 + \frac{1}{2}I\omega^2 \quad (4)$$

where,  $m$  is the mass of the segment  
 $g$  is the gravitational constant  
 $h$  is the height of the centre of mass of the segment  
 $v$  is the velocity of the centre of mass of the segment  
 $I$  is the moment of inertia relative to the centre of mass of the segment  
 $\omega$  is the angular velocity of the segment

The rate of change of energy (RCE) of each segment was then calculated by the central finite difference equation:

$$RCE_n = [E_{i_{n+1}} - E_{i_{n-1}}] / 2\Delta t \quad (5)$$

where,  $\Delta t$  is the time interval between data points  
 $n$  is the frame count

### **3.5 Model Development**

Two modifications were made to the traditional foot model. As explained in the following sections, these modifications were the addition of a more distal forefoot segment and an relocation of the ankle marker position. These modifications were done individually and then in combination, resulting in a total of four different foot models. Total segment power (TSP) and segment rate of change of energy (RCE) calculations were performed for each of the four models. The four models are as follows; 4-Link model, 5-Link model, 4-Link(ankle) model, and 5-Link(ankle) model

#### **3.5.1 Addition of Forefoot Segment**

The traditional foot model will be referred to as the 4-Link model and is illustrated in Figure 2a. The foot power for the 4-Link model is expressed as the sum of the proximal joint and muscle powers. The addition of a forefoot segment adds an additional link to the system, and is therefore referred to as the 5-Link model (Figure 2b). The foot power for the 5-Link model is expressed as the sum of the proximal joint and muscle powers and the distal joint and muscle powers. The forefoot power involves only the sum of the proximal joint and muscle powers.

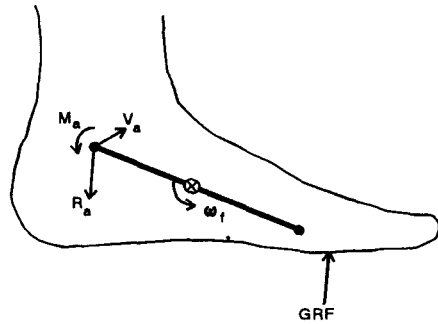
**Figure 2.** Total Segment Power Calculations:  
4-Link Model Foot versus 5-Link Model Foot

- (a) Shows the TSP calculations for the foot in the traditional 4-Link Model
- (b) Shows the TSP calculations for the foot and the forefoot in the 5-Link Model

**Key:**

TSP	total segment power
JP	joint power
MP	muscle power
R	joint reaction force
V	linear velocity of joint
M	moment of force
$\omega$	angular velocity of the segment
prox	denotes the proximal end of the segment
dist	denotes the distal end of the segment
a	denotes the ankle joint
mp	denotes the metatarsal-phalangeal joint
f	denotes the foot segment
ff	denotes the forefoot segment

(a)  
4-LINK FOOT MODEL



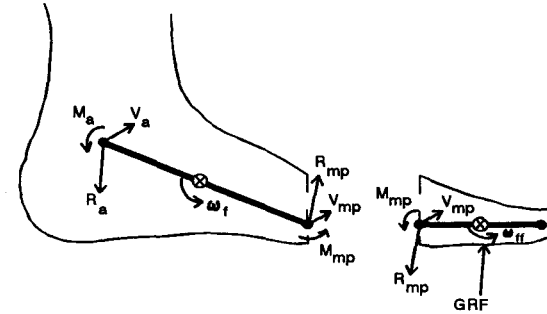
FOOT POWER

$$TSP = [JP + MP]_{prox}$$

$$JP_{prox} = \vec{R}_a \cdot \vec{V}_a$$

$$MP_{prox} = M_a \cdot \omega_f$$

(b)  
5-LINK FOOT MODEL



FOOT POWER

$$TSP = [JP + MP]_{prox} + [JP + MP]_{dist}$$

$$JP_{prox} = \vec{R}_a \cdot \vec{V}_a$$

$$JP_{dist} = \vec{R}_{mp} \cdot \vec{V}_{mp}$$

$$MP_{prox} = M_a \cdot \omega_f$$

$$MP_{dist} = M_{mp} \cdot \omega_{ff}$$

FOREFOOT POWER

$$TSP = [JP + MP]_{prox}$$

$$JP_{prox} = \vec{R}_{mp} \cdot \vec{V}_{mp}$$

$$MP_{prox} = M_{mp} \cdot \omega_{ff}$$

### 3.5.2. Modification of Ankle Joint Position

In order to decrease foot segment length variability, the position of the ankle marker was relocated to extend the leg segment. This position was determined by extending the leg segment in increments of 1mm, for a minimum distance of 0mm to a maximum distance of 50mm, and calculating the standard deviation of the foot segment length throughout the movement. The location, which provided the least amount of foot segment length variability, was chosen to represent the ankle joint for each trial. This ankle relocation was incorporated in both the 4-Link and 5-Link models and will be referred to as the 4-Link(ankle) and the 5-Link(ankle) models, respectively.

## 3.6 Statistical Measures

### 3.6.1 Comparison of Models

Pearson's product-moment correlation coefficients ( $r$ ) were used to correlate the TSP with the RCE as a time series for each trial.  $r$ -values were calculated using equation (6).

$$r = \frac{\sum (TSP * RCE) - (\sum TSP)(\sum RCE)/N}{\left[ \left[ \sum TSP^2 - (\sum TSP)^2/N \right] \left[ \sum RCE^2 - (\sum RCE)^2/N \right] \right]^{1/2}} \quad (6)$$

where,  $N$  is the number of data points in the time series

Percent root mean square error (%RMS) was used to assess the magnitude of the discrepancy between these two methods. The %RMS error was expressed as a percentage of the total rate of change of energy (RCE) of the segment. %RMS was calculated using equation (7).

$$\%RMS = \frac{[(\sum (TSP_n - RCE_n)^2)/N]^{1/2}}{[(\sum (RCE_n)^2)/N]^{1/2}} * 100\% \quad (7)$$

where, N is the number of data points in the time series

Difference scores for both the correlation coefficients and the %RMS error scores were used to assess the magnitude of the differences between models.

### 3.6.2. Assessment of Foot Length Variability

Foot length was calculated for each time point throughout each trial for both the original ankle position and the relocated ankle position. Segment length variability was expressed as a percentage of the range divided by the mean foot length for each of the CMJ and SQJ conditions.

Pearson's product-moment correlations were performed between the segment length and the ankle angular displacement for each trial, to assess the relationship between the segment length and the degree of dorsiflexion or plantarflexion of the ankle complex.

## Chapter 4

### Results

#### 4.1 Foot Anthropometrics

The measured forefoot parameters are presented in Table 3. These measures were used to calculate anthropometric values for the forefoot segment. The calculated segment masses, centres of mass and radii of gyration for the forefoot and hindfoot can be found in Table 2 (Chapter 3, p. 15). Measured and calculated subject foot anthropometrics are included in Appendix A.

**Table 3 Measured Forefoot Parameters**

Parameter	Males		Females	
	Mean	SD	Mean	SD
Forefoot Volume (cm <sup>3</sup> )	180.8	25.0	137.1	19.9
Forefoot Mass* (kg)	0.199	0.028	0.151	0.022
Forefoot Mass (%TBM)	0.239	0.015	0.226	0.031
Forefoot Length (cm)	9.6	0.9	9.2	0.3
Forefoot Breadth (cm)	10.7	0.8	9.4	0.3

TBM = total body mass; SD = standard deviation

\* calculated from forefoot volume (foot density from Dempster via Winter (1990))

## 4.2 Model Development

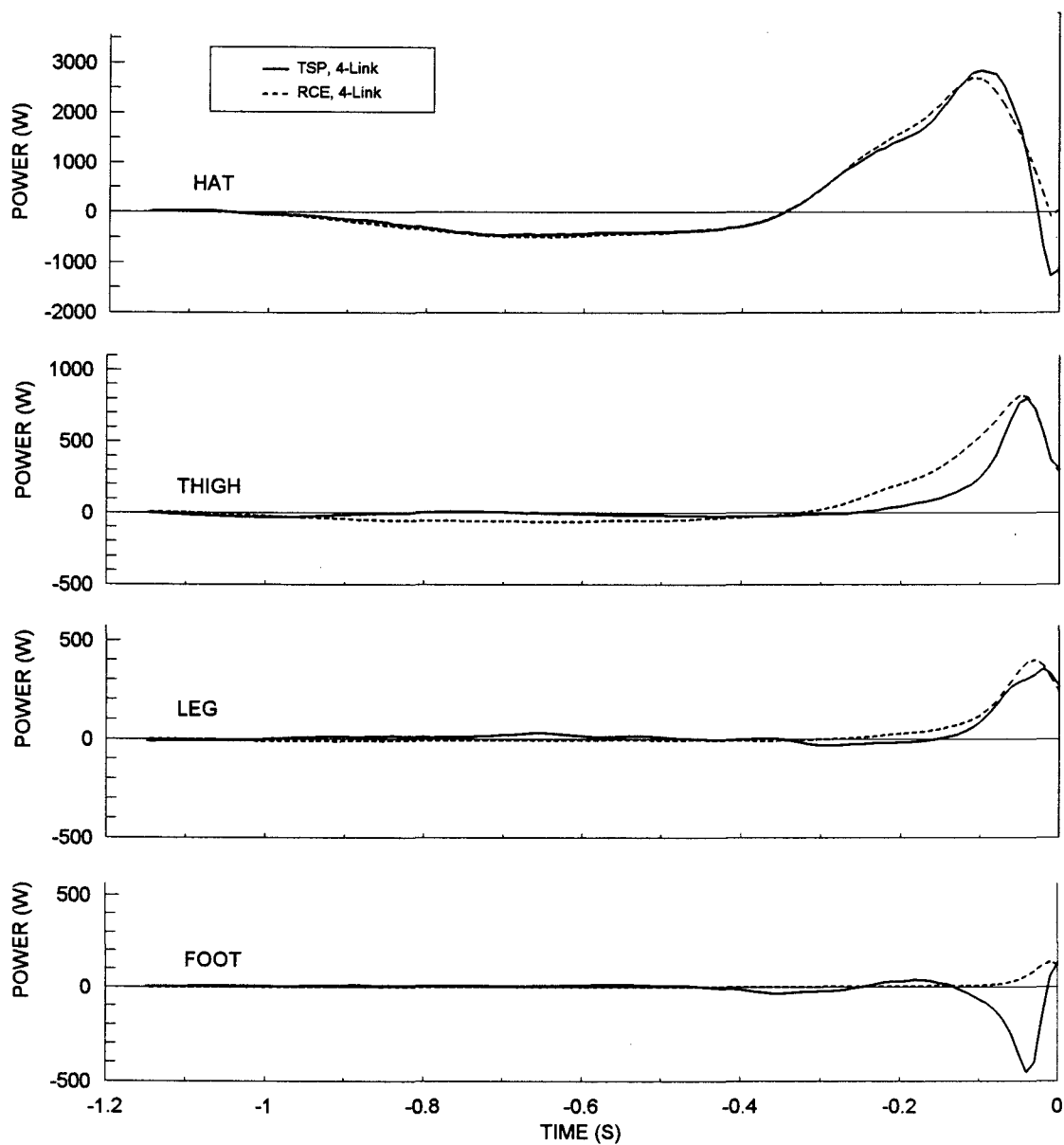
Results are presented according to the model development process. This process began by first calculating the TSP and RCE values for all segments in the 4-Link model. Substantial differences between the TSP and RCE were found for the foot segment of this model. It was hypothesized that the addition of a forefoot segment to the 4-Link model would account for the differences, and if so, the resulting 5-Link model would allow an investigation of the contribution of forefoot segment power to the vertical jump. Further development was required however, as the 5-Link foot model did not resolve all of the differences between the TSP and the RCE for the foot segment.

Changes in foot segment length during the jumping motion were detected and examined as a possible contributor to the TSP and RCE differences. Closer examination showed substantial lengthening of the foot segment length with plantarflexion, and shortening of the foot segment length with dorsiflexion during the jumping trials. To address this problem, the ankle joint location was modified. This modification involved a relocation of the ankle joint to a position which minimized the segment length variability, thus creating the 4-Link(ankle) and 5-Link(ankle) models. It was found that the 5-Link(ankle) model provided a good match between the TSP and RCE for the foot segment.

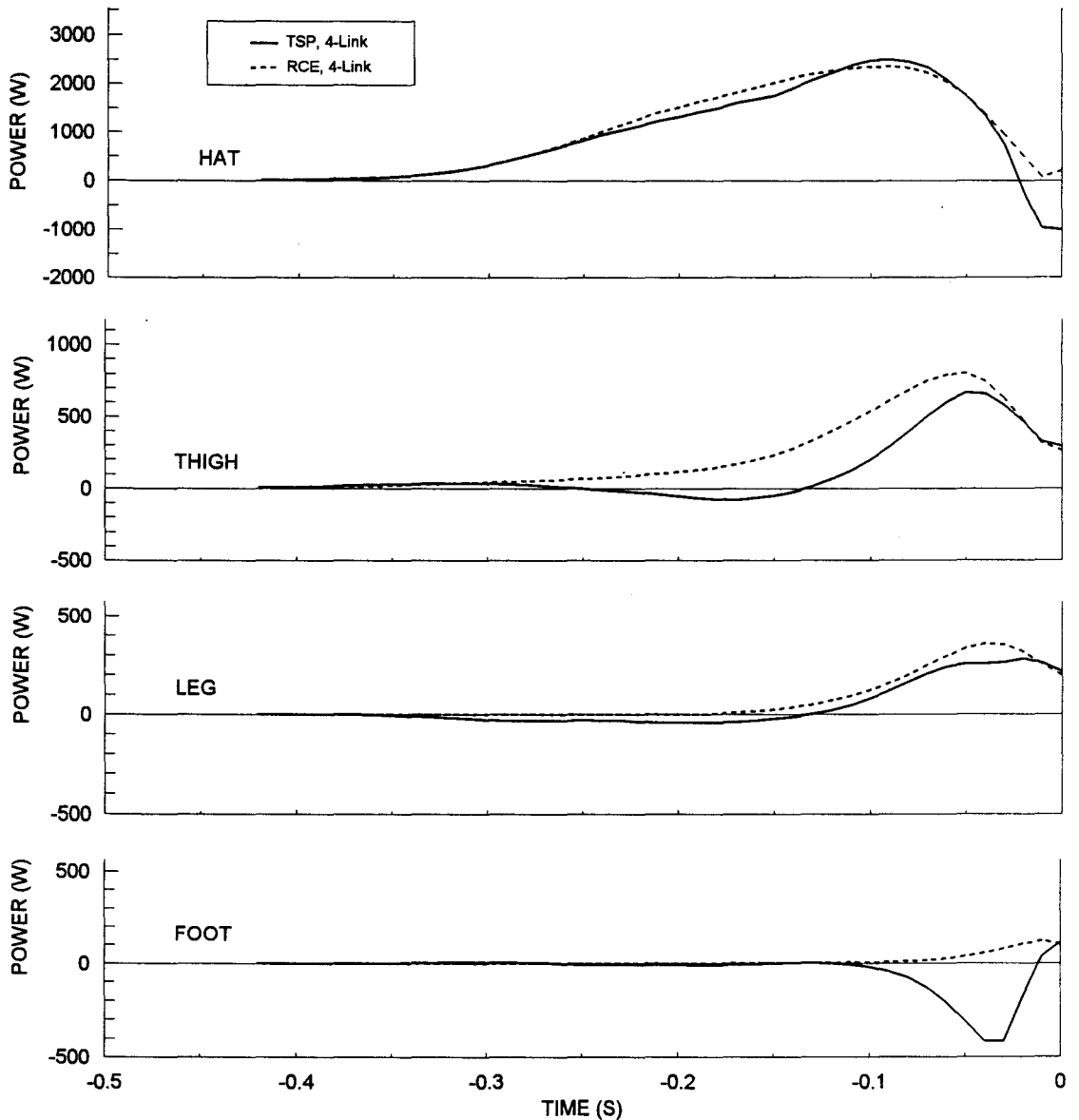
#### 4.2.1 Traditional 4-Link Model

Figure 3 and 4 illustrate the typical differences between TSP and RCE for all segments in the 4-Link model for a CMJ and SQJ, respectively. Takeoff occurred at time zero. Substantial differences between the two curves occur just before takeoff for the foot segment. This discrepancy, displayed by all subjects, was characterized by a large negative deflection of the TSP curve, while the RCE curve deflected positively.

Correlation coefficients and %RMS error scores were calculated over time, comparing the TSP and the RCE for all segments, for all subjects. Group means and standard deviations are reported in Table 4 and Table 5.



**Figure 3.** 4-Link Model Total Segment Power (TSP) and Rate of Change of Energy (RCE) Curve Comparison for All Segments of a Typical Subject (M1) for a CMJ



**Figure 4.** 4-Link Model Total Segment Power (TSP) and Rate of Change of Energy (RCE) Curve Comparison for All Segments of a Typical Subject (M1) in a SQJ

**Table 4 4-Link Model Correlation Coefficients for TSP and RCE**

Segment		CMJ		SQJ	
		Mean	SD	Mean	SD
Foot	M	-0.46	0.05	-0.48	0.09
	F	-0.50	0.10	-0.45	0.12
Leg	M	0.88	0.06	0.89	0.12
	F	0.76	0.15	0.87	0.09
Thigh	M	0.95	0.03	0.94	0.03
	F	0.96	0.02	0.95	0.03
HAT	M	0.99	0.01	0.97	0.01
	F	0.98	0.01	0.97	0.01

CMJ = counter-movement jump; SQJ = squat jump  
M = male; F = female; SD = standard deviation

**Table 5 4-Link Model %RMS Error for TSP and RCE**

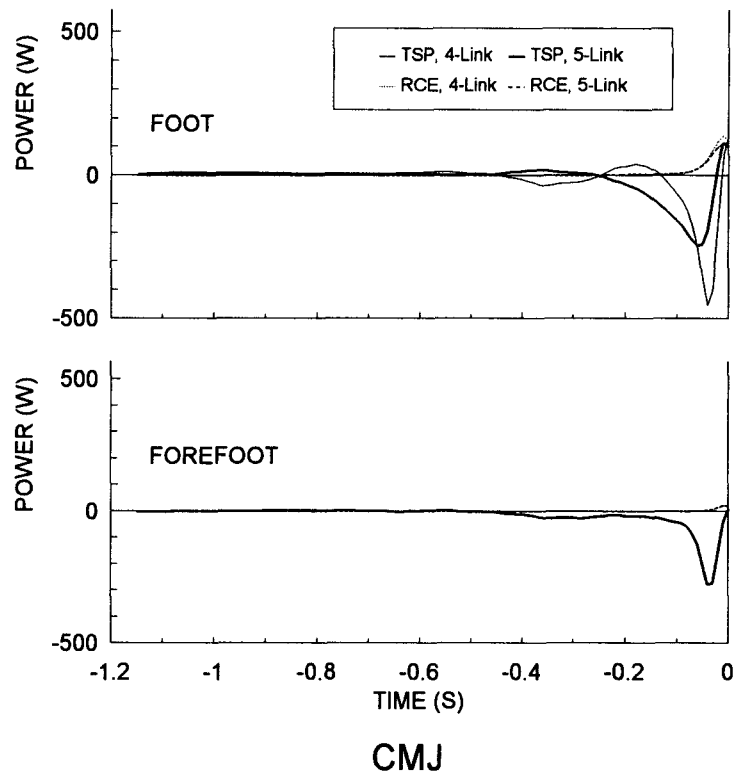
Segment		CMJ		SQJ	
		Mean	SD	Mean	SD
Foot	M	380.5	45.6	425.8	85.1
	F	466.9	70.1	417.0	78.3
Leg	M	44.5	10.3	44.9	18.0
	F	59.8	19.4	51.3	17.7
Thigh	M	33.6	8.2	33.2	8.8
	F	31.5	7.5	33.2	10.2
HAT	M	16.3	3.0	18.0	3.1
	F	19.1	5.4	19.3	5.4

CMJ = counter-movement jump; SQJ = squat jump  
M = male; F = female; SD = standard deviation

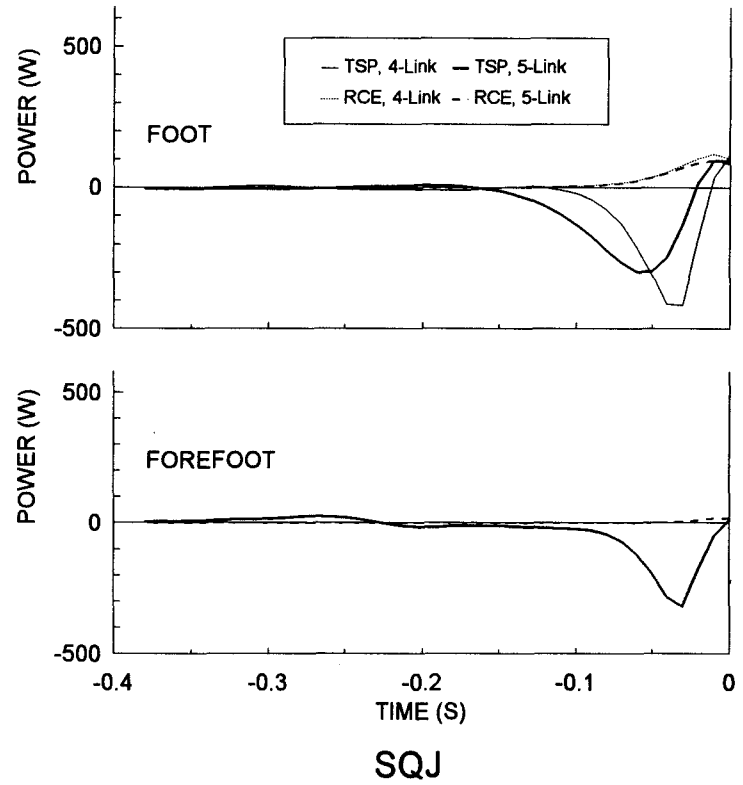
#### 4.2.2 Addition of Forefoot Segment

The first modification to the traditional model was the addition of a fifth segment, called the forefoot. Figures 5a and 5b illustrate typical TSP and RCE curves for the foot and forefoot segments for a CMJ and a SQJ, respectively.

For the foot segment, the negative deflection of the TSP curve for the 5-Link model had a decreased amplitude and a decreased frequency as compared to the TSP curve for the 4-Link model (Figure 5a and 5b). For the CMJ, correlation coefficients improved from -0.46 to -0.05 for the males and from -0.50 to -0.17 for the females, while %RMS error decreased from 380.5% to 264.4% for the males and decreased slightly 466.9% to 394.7% for the females. For the SQJ, correlation coefficients improved from -0.48 to -0.09 for the males and from -0.45 to -0.18 for the females, while %RMS error decreased slightly from 425.8% to 301.2% for the males but did not change for the females (from 417.0% to 423.3%). Relatively high standard deviations for the %RMS scores for the foot segment should be noted in Tables 5 and 6. Individual subject statistics are presented in section 4.3. Considerable discrepancy between the TSP and RCE curves was still present after the addition of the forefoot segment to the traditional foot model. Statistics for the foot segment in the 5-Link model are shown in Table 6.



(a)



(b)

**Figure 5.** 5-Link Model Total Segment Power (TSP) and Rate of Change of Energy (RCE) Curve Comparison for the Foot and Forefoot Segments of a Typical Subject (M1) for a CMJ (a) and a SQJ (b).

**Table 6 5-Link Model Statistics for the Foot Segment**

Statistic		CMJ		SQJ	
		Mean	SD	Mean	SD
Correlation Coefficient	M	-0.05	0.09	-0.09	0.13
	F	-0.17	0.13	-0.18	0.09
%RMS	M	264.4	39.4	301.2	56.7
	F	394.7	93.7	423.3	70.9

CMJ = counter-movement jump; SQJ = squat jump  
M = male; F = female; SD = standard deviation

The discrepancy between the TSP and RCE curves for the forefoot segment was similar to that which occurred for the foot segment in the 4-Link model (Figures 5a and 5b). Statistics for the forefoot segment in the 5-Link model (Table 7) reveal a large discrepancy between TSP and RCE, caused by the very small values of the RCE for the forefoot segment (Figure 5a and 5b). Group values for the peak forefoot power are reported in Table 8 and occurred very late in the movement.

**Table 7 5-Link Model Statistics for the Forefoot Segment**

Statistic		CMJ		SQJ	
		Mean	SD	Mean	SD
Correlation Coefficient	M	-0.39	0.08	-0.39	0.04
	F	-0.42	0.10	-0.36	0.11
%RMS	M	2293.3	410.6	2284.8	450.4
	F	2443.6	370.8	2247.9	461.0

CMJ = counter-movement jump; SQJ = squat jump  
M = male; F = female; SD = standard deviation

**Table 8 Peak Forefoot Segment Power**

		CMJ		SQJ	
		Mean	SD	Mean	SD
Peak Forefoot RCE (Watts)	M	27.1	7.2	23.9	6.8
	F	14.6	5.7	12.3	3.8

CMJ = counter-movement jump; SQJ = squat jump  
M = male; F = female; SD = standard deviation

#### 4.2.3 Ankle Location and its Effect on Foot Segment Length

Foot length changes during the jumping motion are evident in Figure 6a and 6c. Lengthening of the foot segment occurred as the ankle complex plantarflexed (Figures 6a,b; 6c,d) while shortening of the foot segment occurred as the ankle complex dorsiflexed (Figure 6a,b). High correlations between the foot length and ankle angle are presented in Table 9. Ankle angle was defined as the anterior angle between the foot and leg segments.

**Table 9 Correlation of Foot Length with Ankle Angle**

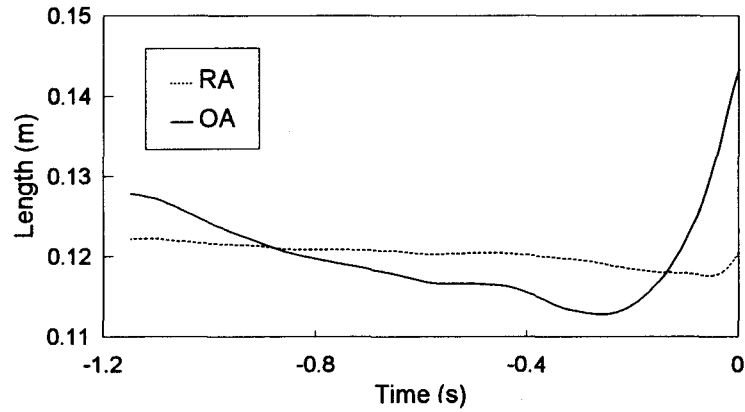
		CMJ		SQJ	
		Mean	SD	Mean	SD
Correlation Coefficient	M	0.903	0.139	0.968	0.034
	F	0.868	0.106	0.943	0.103

CMJ = counter-movement jump, SQJ = squat jump  
M = male, F = female; SD = standard deviation

**Figure 6.** Comparison of Foot Length with Ankle Angle for a Typical Subject (M1)

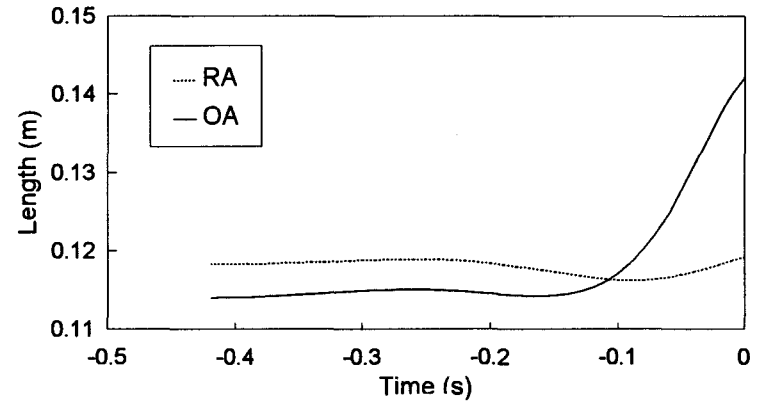
- (a) Comparison of the foot length with original ankle position (OA) with the foot length with relocated ankle position (RA) for a CMJ
- (b) Anterior ankle angle versus time for a CMJ
- (c) Comparison of foot length with original ankle position (OA) with the foot length with the relocated ankle position (RA) for a SQJ
- (b) Anterior ankle angle versus time for a SQJ

**FOOT LENGTH: CMJ**



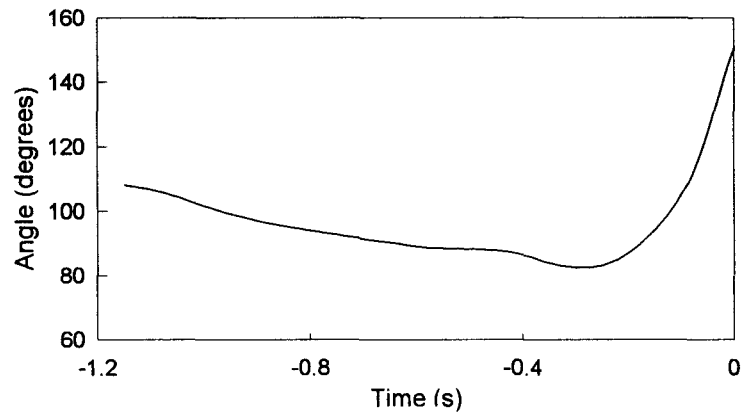
(a)

**FOOT LENGTH: SQJ**



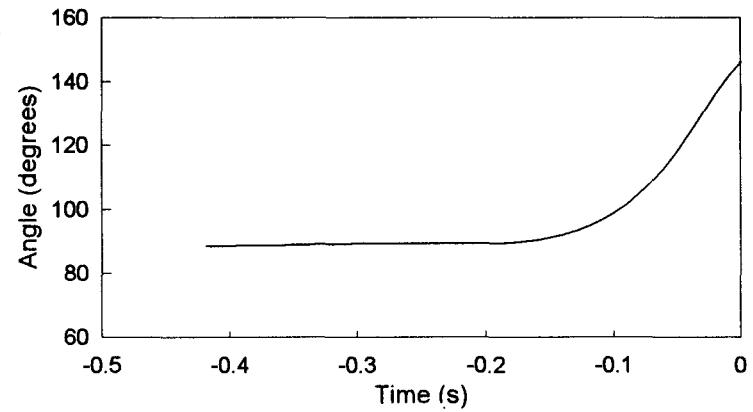
(c)

**ANKLE ANGLE: CMJ**



(b)

**ANKLE ANGLE: SQJ**



(d)

Ankle marker positions were relocated between 16mm and 32mm for all subjects, except for one female subject who required a 50mm relocation. Group means and standard deviations of the distance the leg was extended are presented in Table 10. Figures 6a and 6c show that the foot length remained more stable after ankle joint relocation. Table 11 illustrates that the segment length variability decreased substantially with ankle relocation. This variability was expressed as a percentage of the range divided by the mean.

**Table 10 Ankle Marker Relocation Distance**

		CMJ		SQJ	
		Mean	SD	Mean	SD
Ankle Relocation (mm)	M	25	4.3	23	4.8
	F	28	9.9	26	4.8

CMJ = counter-movement jump, SQJ = squat jump  
M = male, F = female; SD = standard deviation

**Table 11 Segment Length Variability (Range/Mean \* 100%)**

Segment		CMJ		SQJ	
		Mean	SD	Mean	SD
Foot (Original Ankle)	M	21.4	3.3	19.1	5.8
	F	22.4	5.7	22.8	1.9
Foot (Relocated Ankle)	M	5.3	2.8	3.2	1.5
	F	7.0	5.6	4.0	2.5

CMJ = counter-movement jump; SQJ = squat jump  
M = male; F= female; SD = standard deviation

#### 4.2.4 Modification of Ankle Joint Position

The TSP and RCE curves for the 4-Link(ankle) model in the CMJ and SQJ are presented in Figures 7b and 8b, respectively. When compared to the 4-Link model (Figures 7a, 8a), the 4-Link(ankle) model shows a marked positive deflection of the TSP curve followed by a more narrow negative deflection just before takeoff (Figures 7b, 8b). For the CMJ, correlation coefficients improved from -0.46 to -0.18 for the males and from -0.50 to -0.14 for the females, while %RMS error decreased from 380.5% to 264.2% for the males and decreased slightly from 466.9% to 379.7% for the females. For the SQJ, correlation coefficients improved from -0.48 to -0.34 for the males and from -0.45 to -0.01 for the females, while %RMS error decreased slightly from 425.8% to 294.2% for the males and from 417.0% to 361.8% for the females. Relatively high standard deviations for the %RMS scores for the foot segment should be noted in Tables 5 and 12. Individual subject statistics are presented in section 4.3. The group mean correlation coefficients and %RMS error scores for the foot segment in the 4-Link(ankle) model are presented in Table 12.

**Figure 7.** Total Segment Power (TSP) and Rate of Change of Energy (RCE) Curve Comparison for the Foot Segment for a Typical Subject (M1) Under the Four Model Conditions for a CMJ.

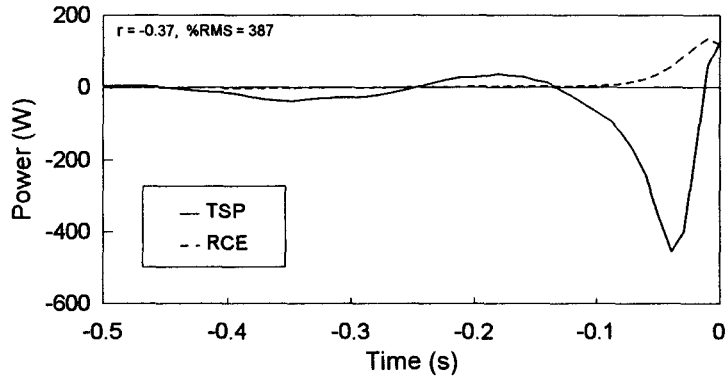
- (a) 4-Link model
- (b) 4-Link(ankle) model
- (c) 5-Link model
- (d) 5-Link(ankle) model

Key:

r Pearson's correlation coefficients between TSP and RCE

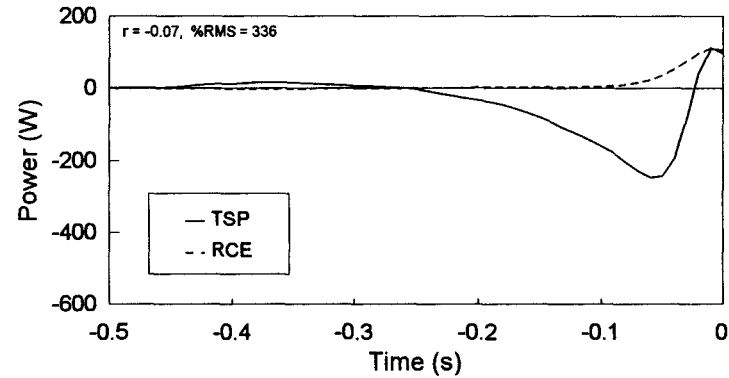
%RMS Percent root mean square error comparing TSP and RCE

### 4-LINK



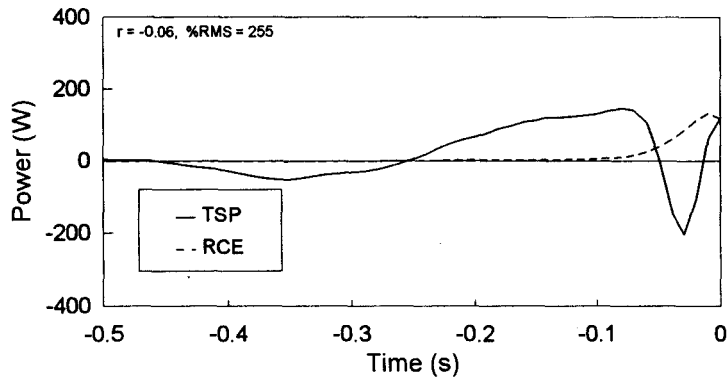
(a)

### 5-LINK



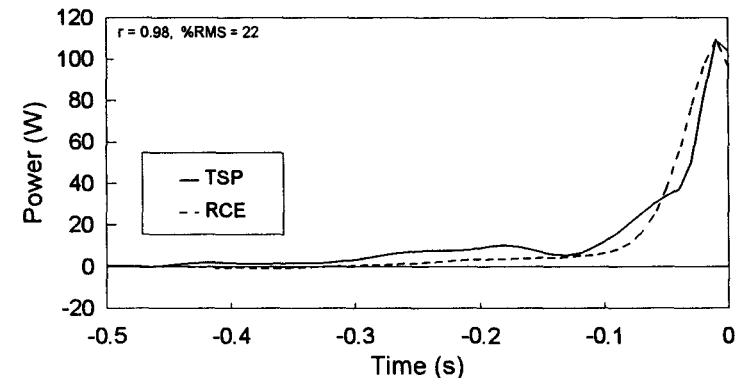
(c)

### 4-LINK(ANKLE)



(b)

### 5-LINK(ANKLE)



(d)

**Figure 8.** Total Segment Power (TSP) and Rate of Change of Energy (RCE) Curve Comparison for the Foot Segment for a Typical Subject (M1) Under the Four Model Conditions for a SQJ.

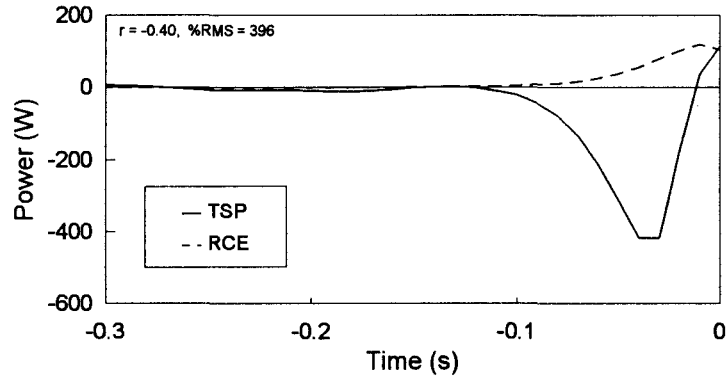
- (a) 4-Link model
- (b) 4-Link(ankle) model
- (c) 5-Link model
- (d) 5-Link(ankle) model

Key:

r                      Pearson's correlation coefficients between TSP and RCE

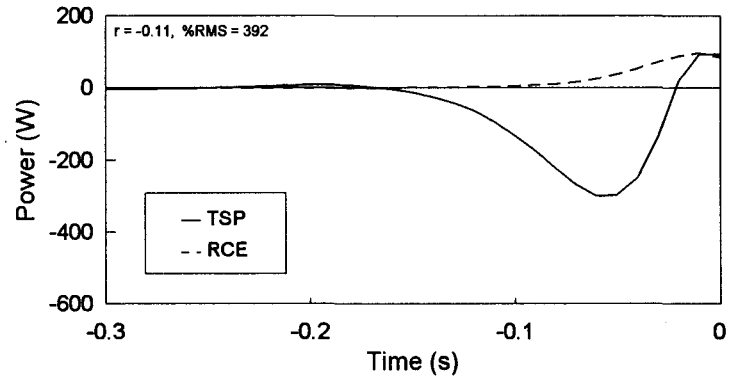
%RMS                Percent root mean square error comparing TSP and RCE

### 4-LINK



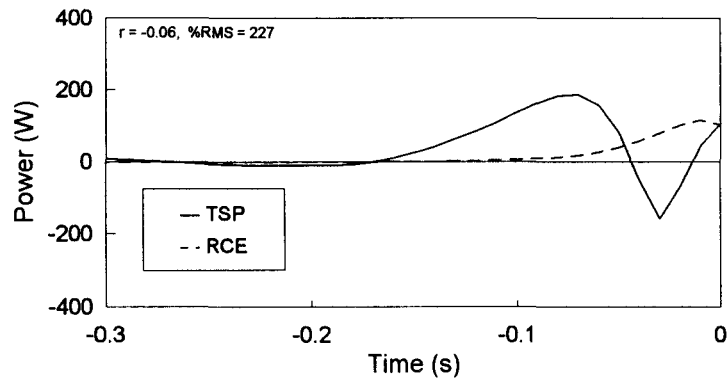
(a)

### 5-LINK



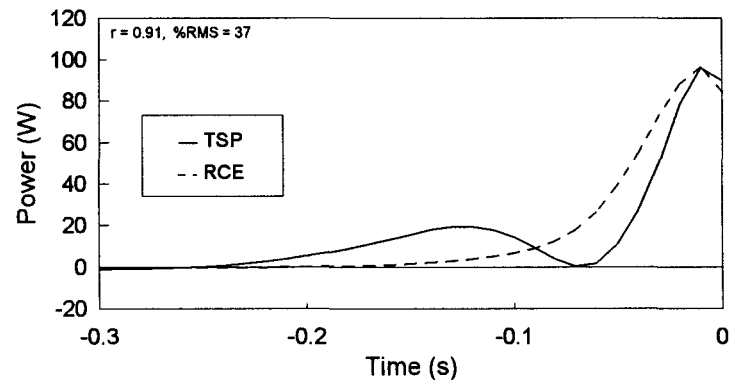
(c)

### 4-LINK(ANKLE)



(b)

### 5-LINK(ANKLE)



(d)

**Table 12 4-Link(ankle) Model Statistics for the Foot Segment**

Statistic		CMJ		SQJ	
		Mean	SD	Mean	SD
Correlation Coefficient	M	-0.18	0.13	-0.34	0.22
	F	-0.14	0.26	-0.01	0.14
-----					
%RMS	M	264.2	45.5	294.2	54.7
	F	379.7	137.6	361.8	102.7

CMJ = counter-movement jump; SQJ = squat jump  
M = male; F = female; SD = standard deviation

The TSP and RCE curves for the 5-Link(ankle) model are presented in Figures 7d and 8d. For this model, the TSP curve follows the RCE curve closely. For the CMJ, correlation coefficients improved from -0.46 to 0.92 for the males and from -0.50 to 0.77 for the females, while %RMS error decreased from 380.5% to 35.4% for the males and from 466.9% to 71.6% for the females. For the SQJ, correlation coefficients improved from -0.48 to 0.87 for the males and from -0.45 to 0.79 for the females, while %RMS error decreased from 425.8% to 43.4% for the males and from 417.0% to 59.9% for the females. Statistics for the foot segment in the 5-Link(ankle) model are included in Table 13. The discrepancy for the forefoot segment in the 5-Link(ankle) model was the same as that found for the forefoot segment in the 5-Link model (see Figures 5a and 5b). The statistics for the forefoot segment in the 5-Link(ankle) model were identical to those found for the 5-Link model (see Table 7).

**Table 13 5-Link(ankle) Model Statistics for the Foot Segment**

Statistic		CMJ		SQJ	
		Mean	SD	Mean	SD
Correlation Coefficient	M	0.92	0.11	0.87	0.11
	F	0.77	0.16	0.79	0.21
%RMS	M	35.4	17.9	43.4	15.9
	F	71.6	29.6	59.9	39.0

CMJ = counter-movement jump; SQJ = squat jump  
M = male; F = female; SD = standard deviation

#### 4.2.5 Model Comparison

Foot segment statistics for each modified model were compared to the traditional 4-Link model. Difference scores were used to quantify the amount of improvement over the traditional model. Table 14 displays the mean difference scores for the correlation coefficients, where a positive difference indicates improvement. The 5-Link(ankle) model demonstrates the best improvement. Table 15 displays the difference scores for %RMS error, where a negative difference indicates an improvement. Substantial improvements were noted for the foot segment (for all subjects) for the 5-Link(ankle) model. The decrease in the %RMS error for the 5-Link(ankle) model ranged from 250% to 540% , when compared to the 4-Link model.

**Table 14 Correlation Coefficient Difference Scores for Model Comparison**

Comparison		CMJ		SQJ	
		Mean	SD	Mean	SD
5-LINK vs 4-LINK	M	0.41	0.09	0.39	0.10
	F	0.33	0.12	0.27	0.13
4-LINK(ankle) vs 4-LINK	M	0.28	0.11	0.13	0.14
	F	0.36	0.25	0.44	0.16
5-LINK(ankle) vs 4-LINK	M	1.38	0.10	1.35	0.16
	F	1.27	0.18	1.24	0.32

CMJ = counter-movement jump; SQJ = squat jump  
M = male; F = female; SD = standard deviation

**Table 15 %RMS Difference Scores for Model Comparison**

Comparison		CMJ		SQJ	
		Mean	SD	Mean	SD
5-LINK vs 4-LINK	M	-116.1	45.9	-124.6	99.6
	F	-72.1	95.8	6.3	68.9
4-LINK(ankle) vs 4-LINK	M	-116.4	40.4	-131.6	67.4
	F	-87.1	127.7	-55.1	106.9
5-LINK(ankle) vs 4-LINK	M	-345.1	48.7	-382.4	91.6
	F	-395.2	63.7	-357.1	67.1

CMJ = counter-movement jump; SQJ = squat jump  
M = male; F = female; SD = standard deviation

### **4.3 Individual Subject Response to Model Modifications**

Tables 16 and 17 illustrate the correlation coefficients ( $r$ ) and %RMS error between the TSP and RCE for the foot segment for each of the models discussed in section 4.2, for the CMJ and SQJ, respectively. Subjects are rank ordered, from best to worst, based on results from the 5-Link(ankle) model. One subject with high correlations (Figures 9 and 10) and one subject with low correlations (Figures 11 and 12) were chosen to illustrate differences. Figures 9 and 10 show the foot segment length changes observed for subject F8, in the CMJ, followed by the TSP and RCE comparison curves for each of the four models. Figures 11 and 12 show the foot segment length changes observed for subject F5, in the CMJ, followed by the TSP and RCE comparison curves for each of the four models.

**Table 16 Individual Statistics for the Foot Segment in all models for the CMJ**

Subject	5-Link(ankle)		4-Link(ankle)		5-Link		4-Link	
	r	%RMS	r	%RMS	r	%RMS	r	%RMS
F8	0.99	18	0.28	168	-0.27	283	-0.54	302
M5	0.98	20	-0.30	303	0.11	214	-0.45	379
M1	0.98	22	-0.06	255	-0.07	336	-0.37	387
M3	0.97	24	-0.13	254	-0.05	244	-0.49	342
M8	0.97	27	-0.03	176	-0.09	216	-0.47	316
M6	0.96	31	-0.01	226	0.00	261	-0.38	393
M2	0.95	32	-0.33	336	-0.03	258	-0.50	438
F2	0.93	41	-0.43	385	-0.05	365	-0.60	504
M4	0.92	52	-0.40	282	-0.08	303	-0.53	455
F7	0.92	57	-0.36	281	-0.02	361	-0.41	525
F6	0.78	113	0.17	641	-0.20	560	-0.43	464
F1	0.74	72	0.06	499	-0.30	500	-0.51	469
F4	0.66	80	-0.11	445	-0.10	298	-0.32	504
M7	0.64	76	-0.09	281	-0.22	283	-0.49	335
F5	0.58	104	-0.42	296	-0.10	334	-0.56	431
F3	0.54	87	-0.27	323	-0.38	459	-0.65	536

CMJ = counter-movement jump; SQJ = squat jump; M = male; F = female; SD = standard deviation  
 --- subjects above dotted line are those with  $r > 0.8$  and %RMS < 60% for the 5-Link(ankle) model

**Table 17 Individual Statistics for the Foot Segment in all models for the SQJ**

Subject	5-Link(ankle)		4-Link(ankle)		5-Link		4-Link	
	r	%RMS	r	%RMS	r	%RMS	r	%RMS
F6	0.99	17	0.15	391	-0.31	476	-0.55	380
M5	0.97	22	-0.41	296	0.02	235	-0.55	394
F2	0.97	38	-0.34	432	-0.04	419	-0.60	484
M8	0.94	32	-0.55	287	-0.31	234	-0.53	440
F8	0.93	33	0.01	285	-0.19	381	-0.51	350
F4	0.92	37	0.07	203	-0.31	266	-0.58	313
M2	0.92	37	-0.50	425	-0.00	278	-0.50	579
M4	0.92	38	-0.71	265	-0.26	377	-0.64	536
M1	0.91	37	-0.06	227	-0.11	392	-0.40	396
M6	0.85	49	-0.07	260	0.08	316	-0.35	297
F3	0.83	50	0.01	385	-0.24	516	-0.42	441
M3	0.81	56	-0.19	288	0.05	259	-0.36	385
F1	0.72	65	0.10	370	-0.15	431	-0.34	348
F7	0.64	95	-0.13	270	-0.09	471	-0.38	560
M7	0.61	77	-0.27	307	-0.15	320	-0.52	381
F5	0.34	145	0.03	558	-0.15	425	-0.24	462

CMJ = counter-movement jump; SQJ = squat jump; M = male; F = female; SD = standard deviation  
 --- subjects above dotted line are those who had  $r > 0.8$  and  $\%RMS < 60\%$  for the 5-Link(ankle) model

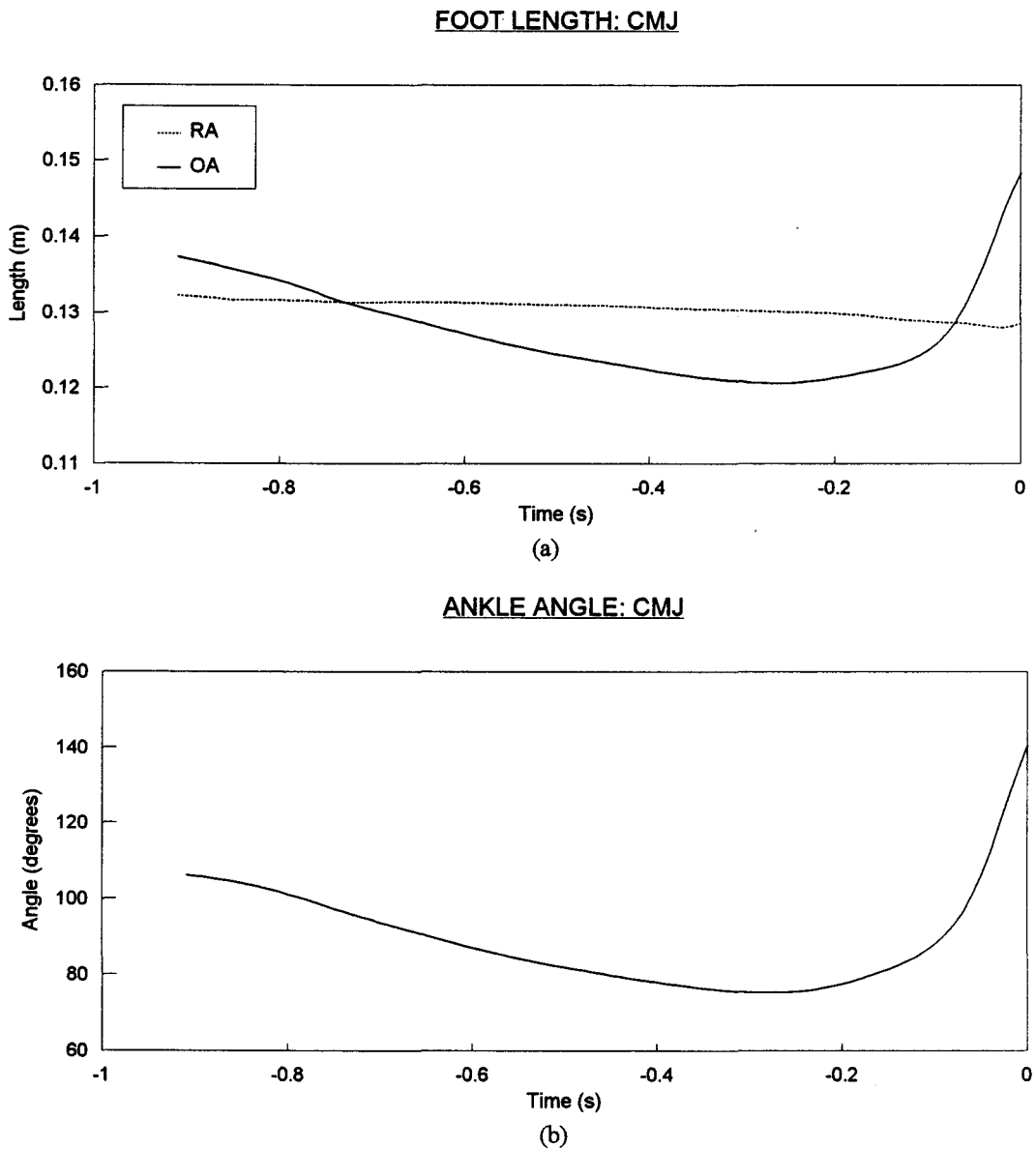


**Figure 9.** Comparison of Foot Length with Ankle Angle for Subject F8 for a CMJ.  
 (a) Comparison of the foot length with original ankle position (OA) with the foot length with relocated ankle position (RA)  
 (b) Anterior ankle angle versus time

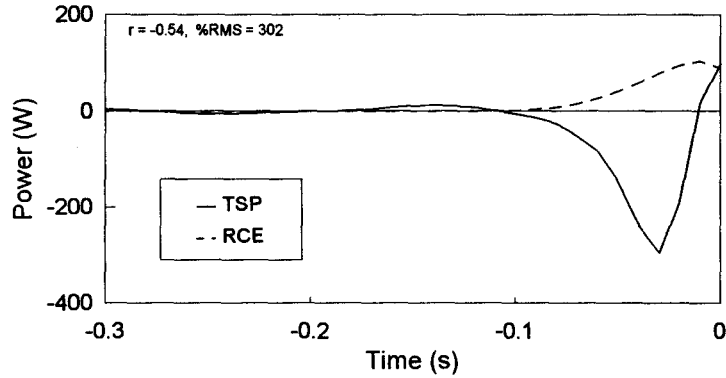
**Figure 10.** Total Segment Power (TSP) and Rate of Change of Energy (RCE) Curve Comparison for the Foot Segment of Subject F8 Under the Four Model Conditions

- (a) 4-Link Model
- (b) 5-Link Model
- (c) 4-Link(ankle) Model
- (d) 5-Link(ankle) Model

**Key:**

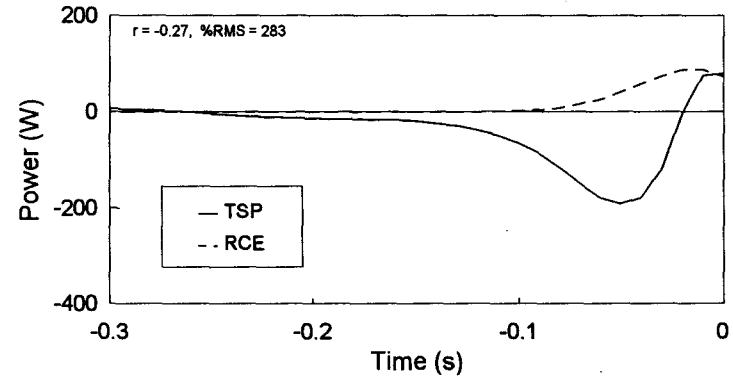
- r Pearson's correlation coefficients between TSP and RCE
- %RMS Percent root mean square error comparing TSP and RCE

### 4-LINK



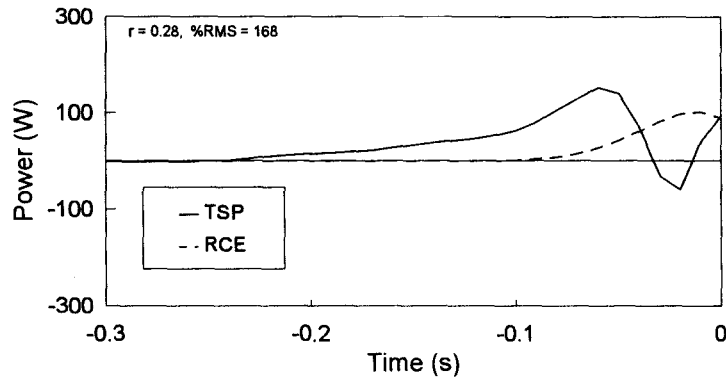
(a)

### 5-LINK



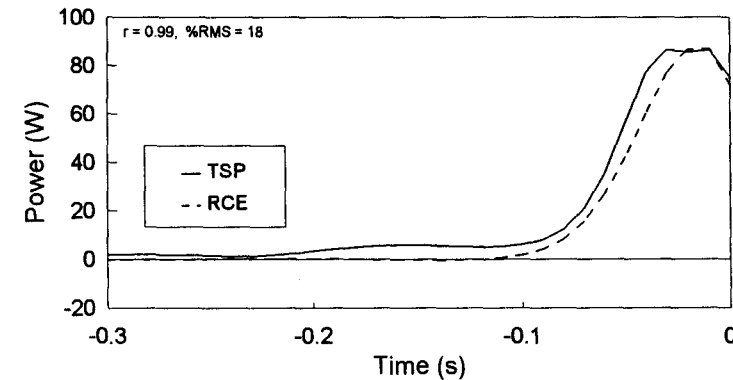
(b)

### 4-LINK(ANKLE)



(c)

### 5-LINK(ANKLE)



(d)

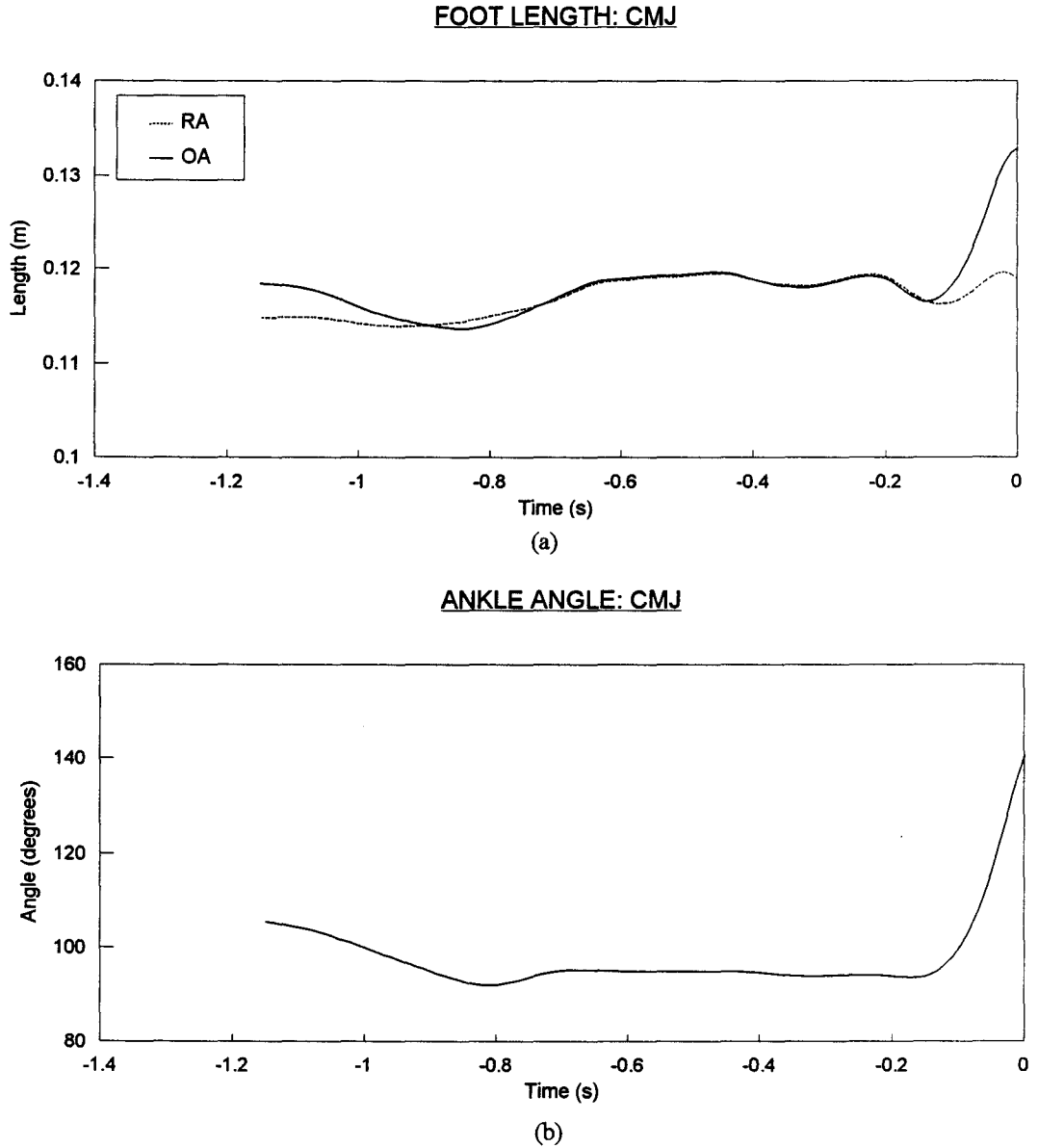


**Figure 11.** Comparison of Foot Length with Ankle Angle for Subject F5 for a CMJ.  
 (a) Comparison of the foot length with original ankle position (OA) with the foot length with relocated ankle position (RA)  
 (b) Anterior ankle angle versus time

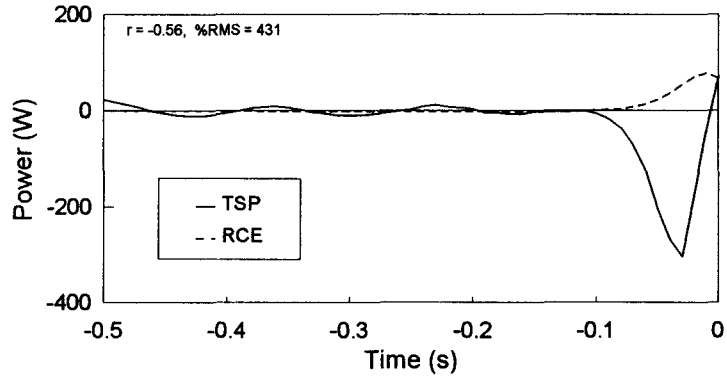
**Figure 12.** Total Segment Power (TSP) and Rate of Change of Energy (RCE) Curve Comparison for the Foot Segment of Subject F5 Under the Four Model Conditions

- (a) 4-Link Model
- (b) 5-Link Model
- (c) 4-Link(ankle) Model
- (d) 5-Link(ankle) Model

Key:

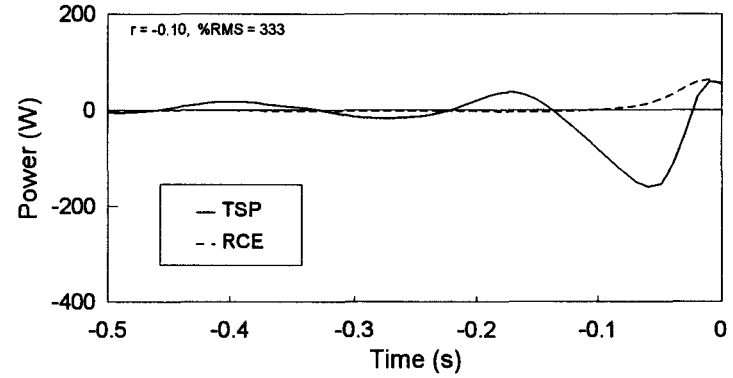
- r Pearson's correlation coefficients between the TSP and RCE
- %RMS Percent root mean square error comparing TSP and RCE

4-LINK



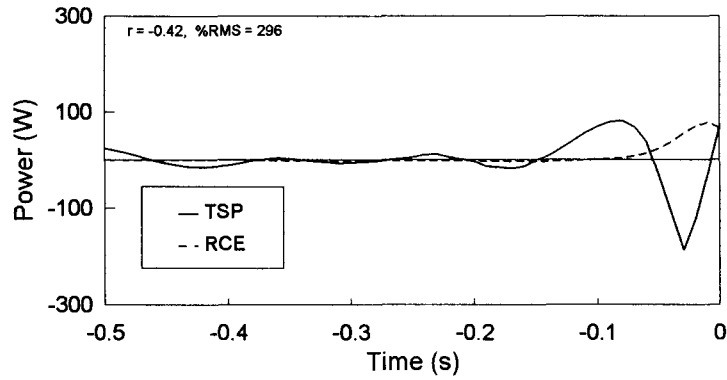
(a)

5-LINK



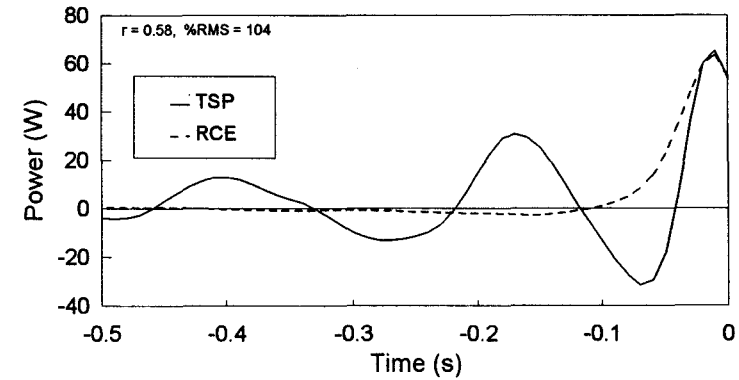
(b)

4-LINK(ANKLE)



(c)

5-LINK(ANKLE)



(d)

#### **4.4 Breakdown of TSP into JP and MP for Model Comparison**

To understand the effect of the different model modifications on the components of the TSP, the following figures are presented for a typical subject (M1). Figure 13 illustrates the TSP and its component joint and muscle powers for each of the 4-Link, 5-Link, 4-Link(ankle) and 5-Link(ankle) models. To illustrate differences between individual components for each model, the ankle joint and muscle powers for each model were graphed in Figures 14 and 16, respectively, and the m-p joint and muscle powers for each model were graphed in Figures 18 and 20, respectively. Figures 15, 17, 19 and 21 show the force/torque and velocity components of the respective joint power or muscle power.

##### **4.4.1 Proximal Power Components (Ankle Joint)**

For the models that incorporated the ankle relocation, the ankle joint power increased slightly (Figure 14). This occurred via a slight increase in the horizontal ankle joint velocity (Figure 15b). Also, the ankle muscle power increased for the 4-Link(ankle) and 5-Link(ankle) models (Figure 16). These changes in ankle muscle power were due to both a change in the ankle moment (Figure 17a), and, a change in the foot segment angular velocity (Figure 17b).

#### 4.4.2 Distal Power Components (M-p Joint)

There was no difference in the m-p joint power between the two models which incorporated a distal joint power term (5-Link, 5-Link(ankle)) (Figure 18). However, there was a decrease in the m-p muscle power for the 5-Link(ankle) model (Figure 20). This change was due to the change in the foot segment angular velocity (Figure 21b) that occurred with ankle relocation.

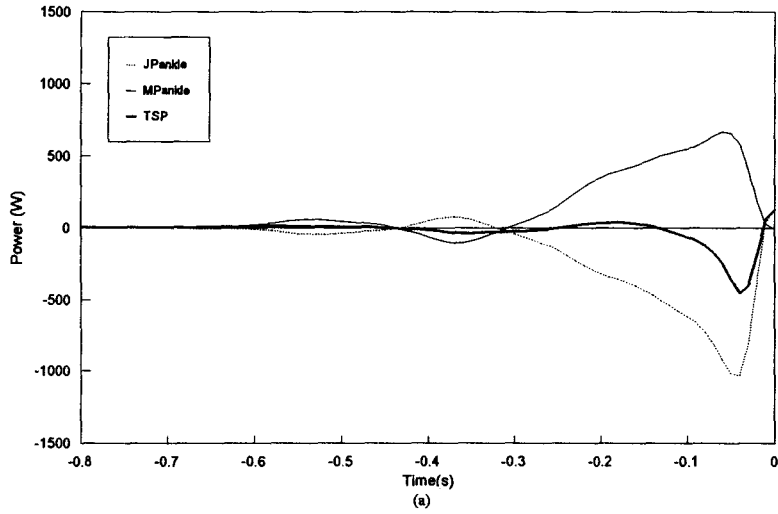
**Figure 13.** Joint Power (JP) and Muscle Power (MP) Components of the Total Segment Power (TSP) for a Typical Subject (M1) Under the Four Model Conditions for a CMJ

- (a) 4-Link Model
- (b) 5-Link Model
- (c) 4-Link(ankle) Model
- (d) 5-Link(ankle) Model

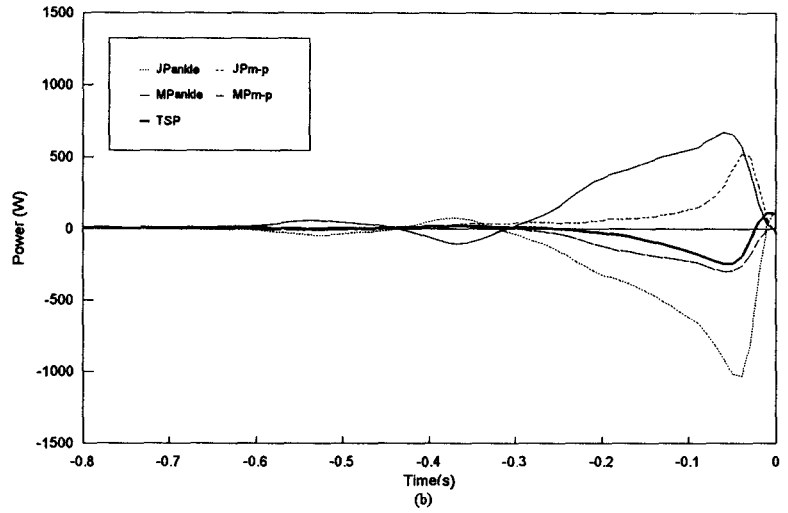
**Key:**

JPankle	Ankle joint power
MPankle	Ankle muscle power
JPm-p	Metatarsal-phalangeal joint power
MPm-p	Metatarsal-phalangeal muscle power
TSP	Total segment power

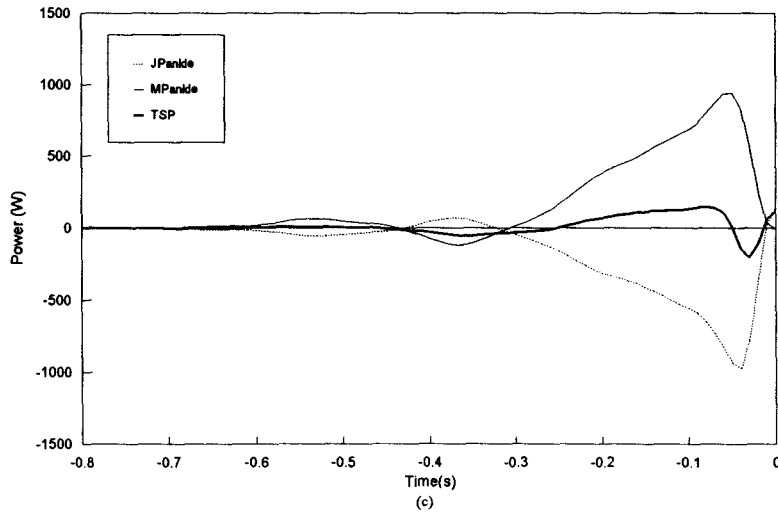
**4-LINK FOOT POWERS**



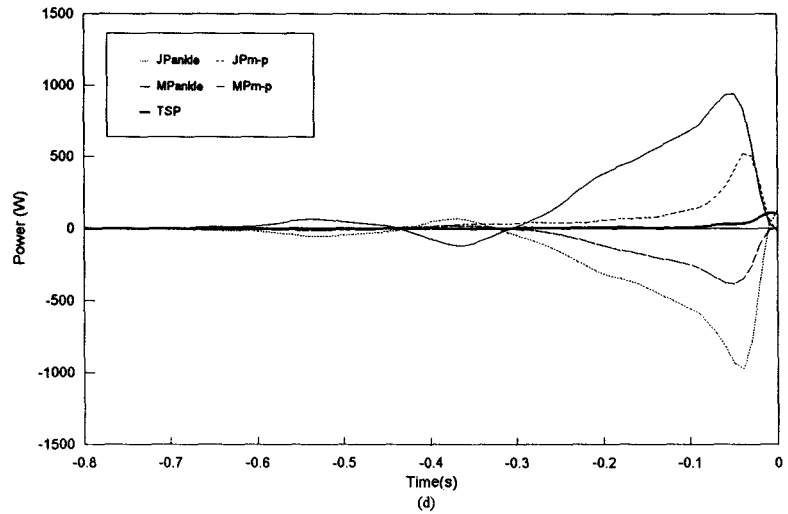
**5-LINK FOOT POWERS**



**4-LINK(ANKLE) FOOT POWERS**



**5-LINK(ANKLE) FOOT POWERS**



### Ankle Joint Power

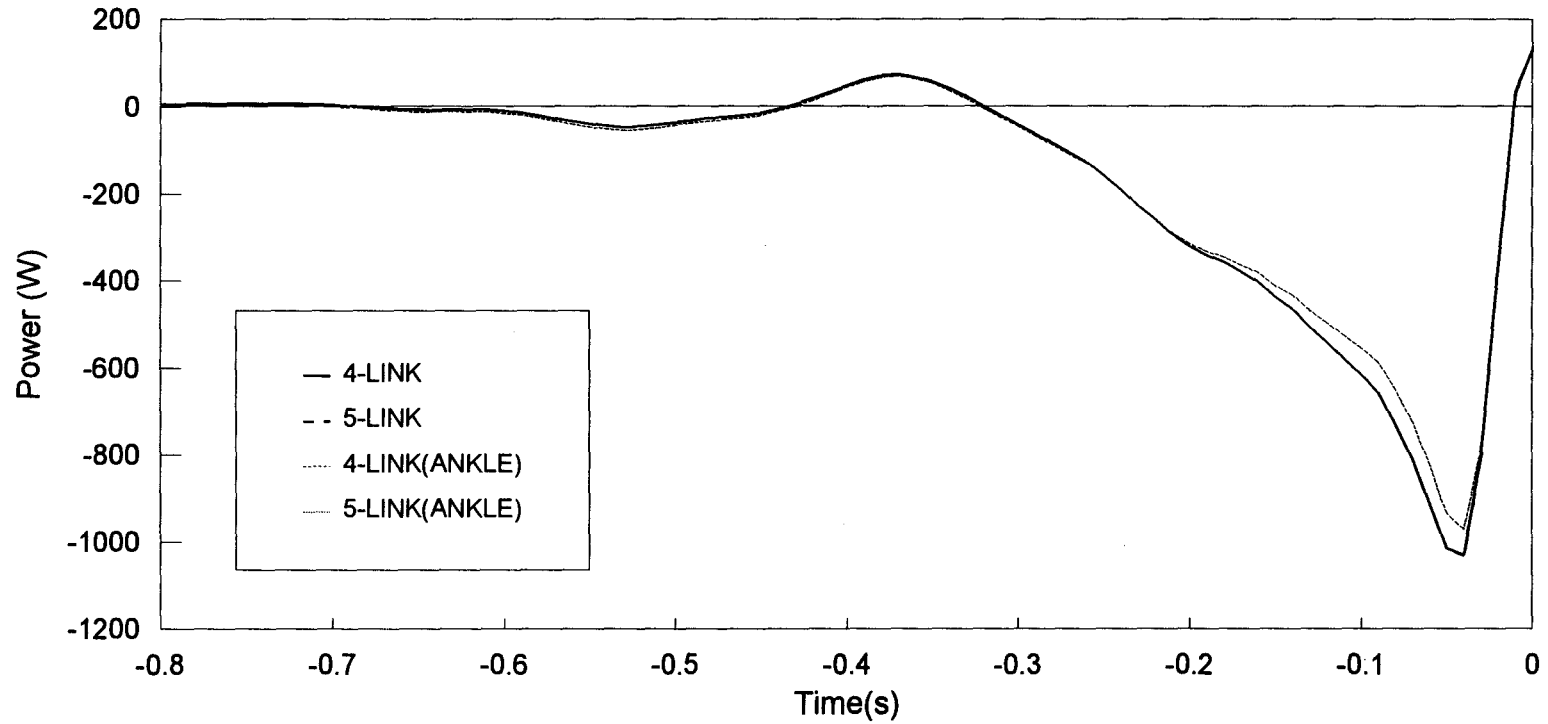


**Figure 14.** Model Comparison of the Ankle Joint Power (JP) for a Typical Subject (M1) for a CMJ

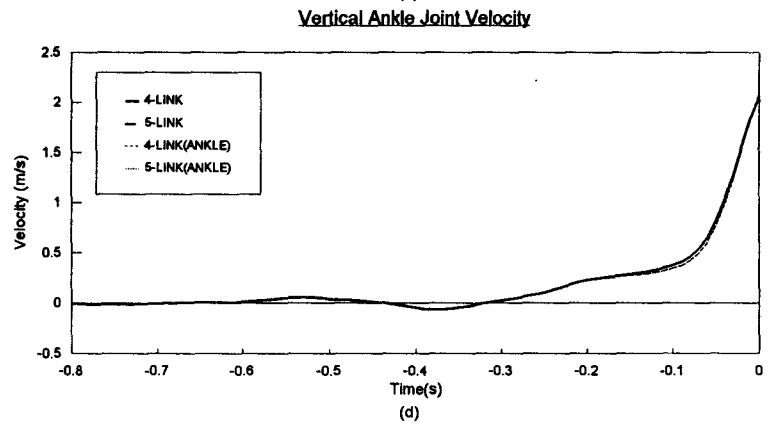
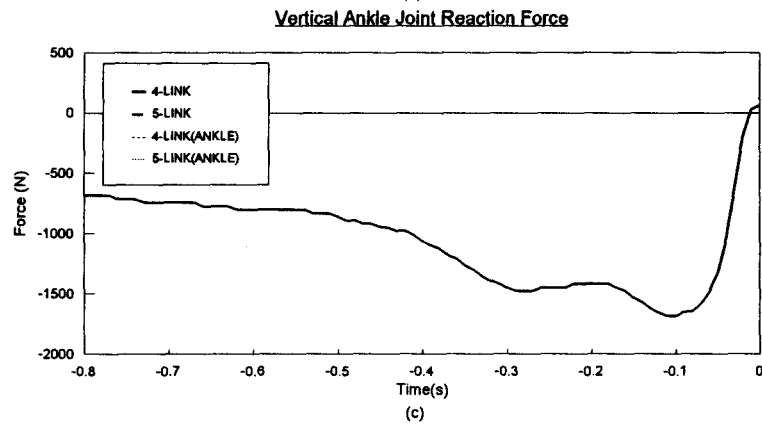
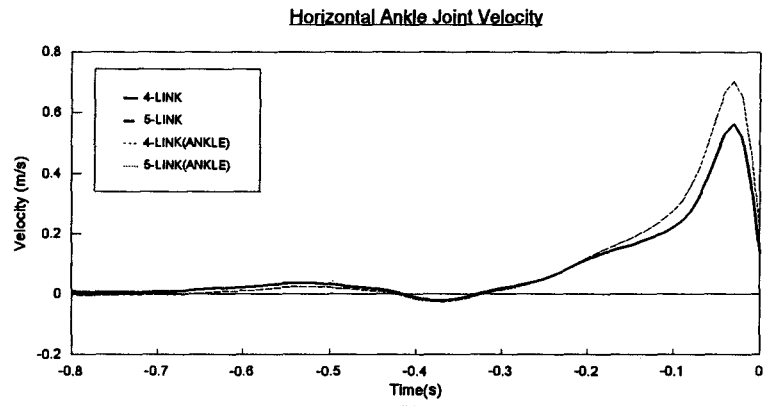
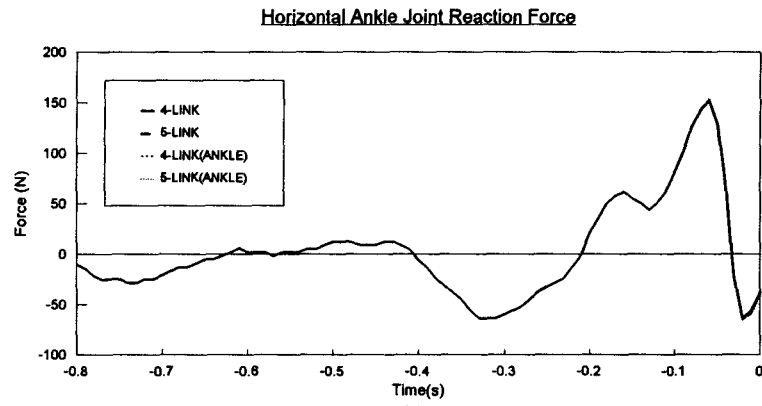


**Figure 15.** Model Comparison of the Ankle Joint Reaction Forces and Ankle Velocities for a Typical Subject (M1) for a CMJ

### Ankle Muscle Power

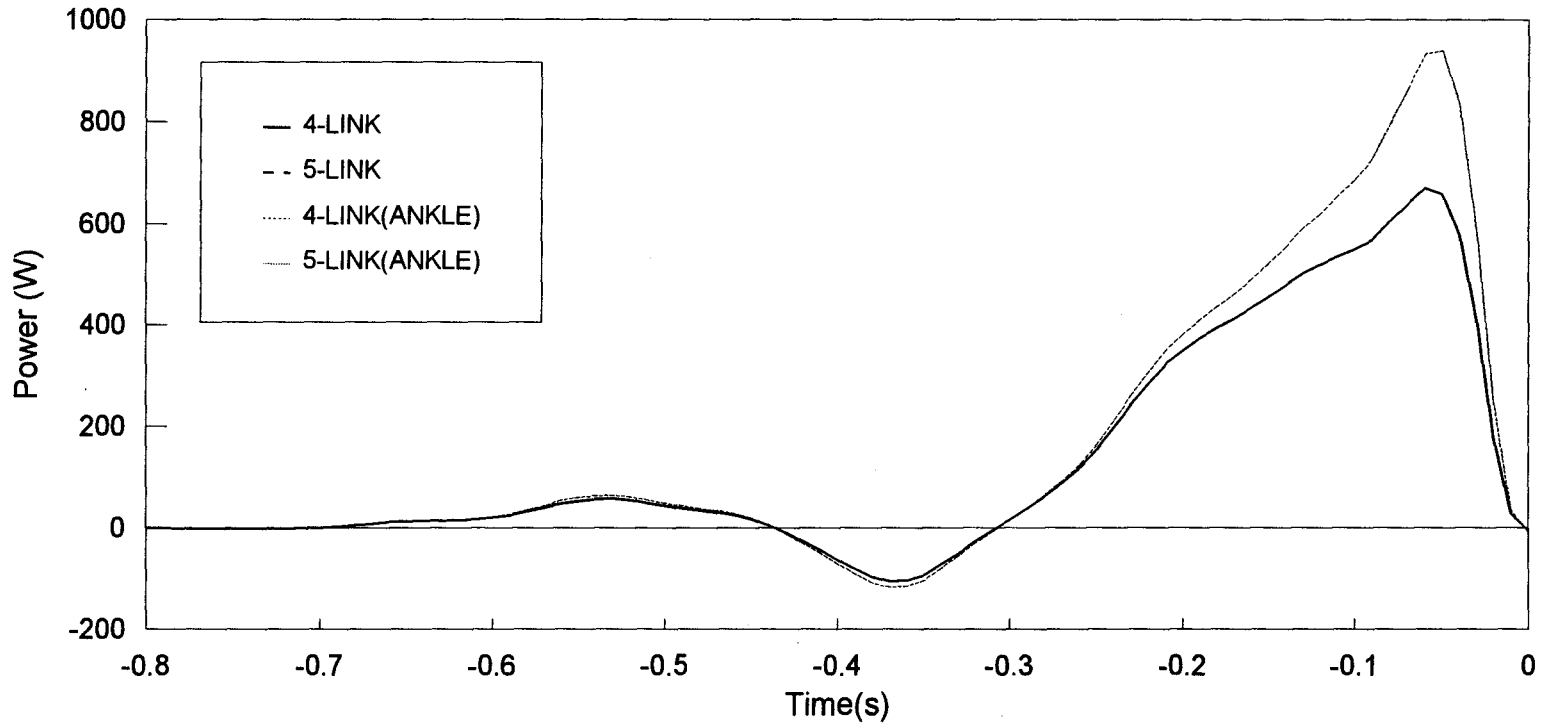
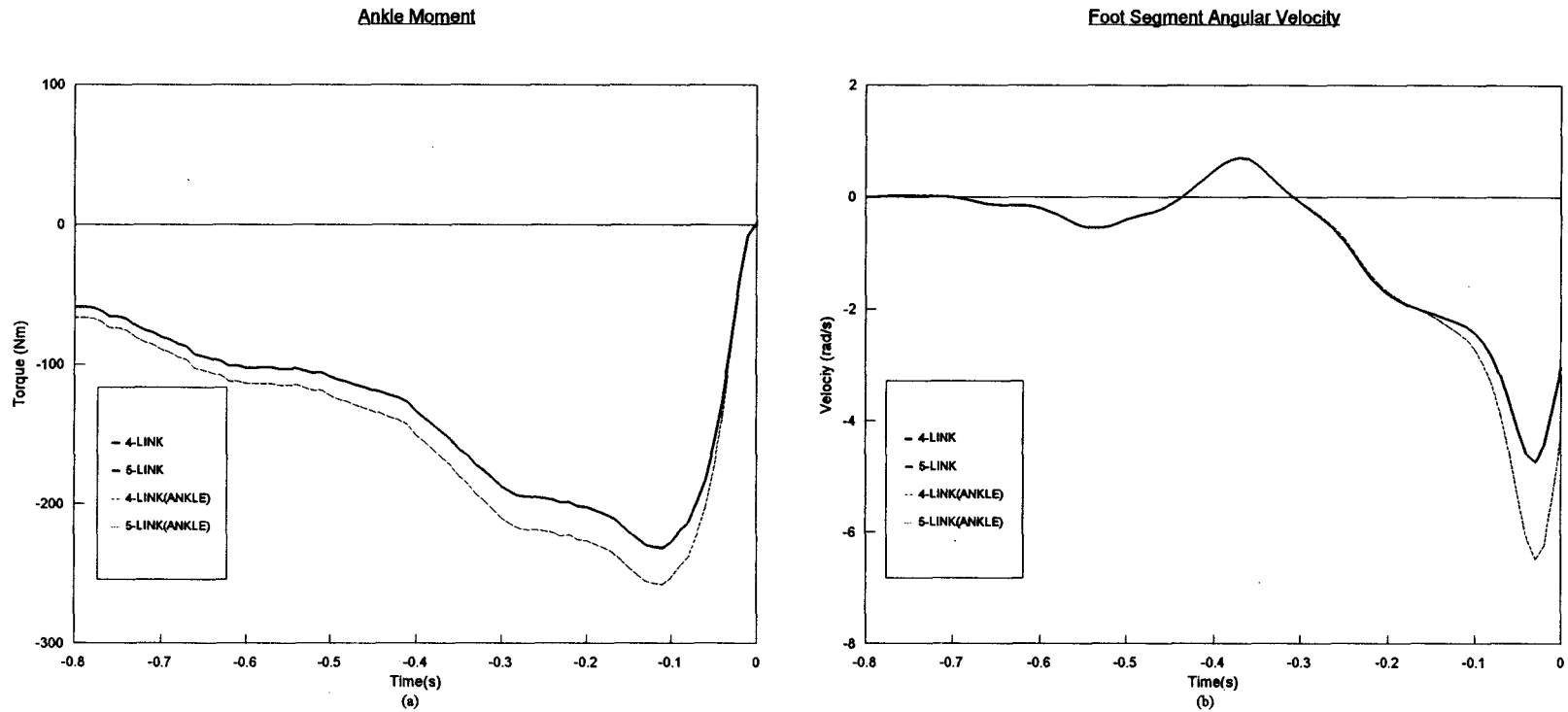
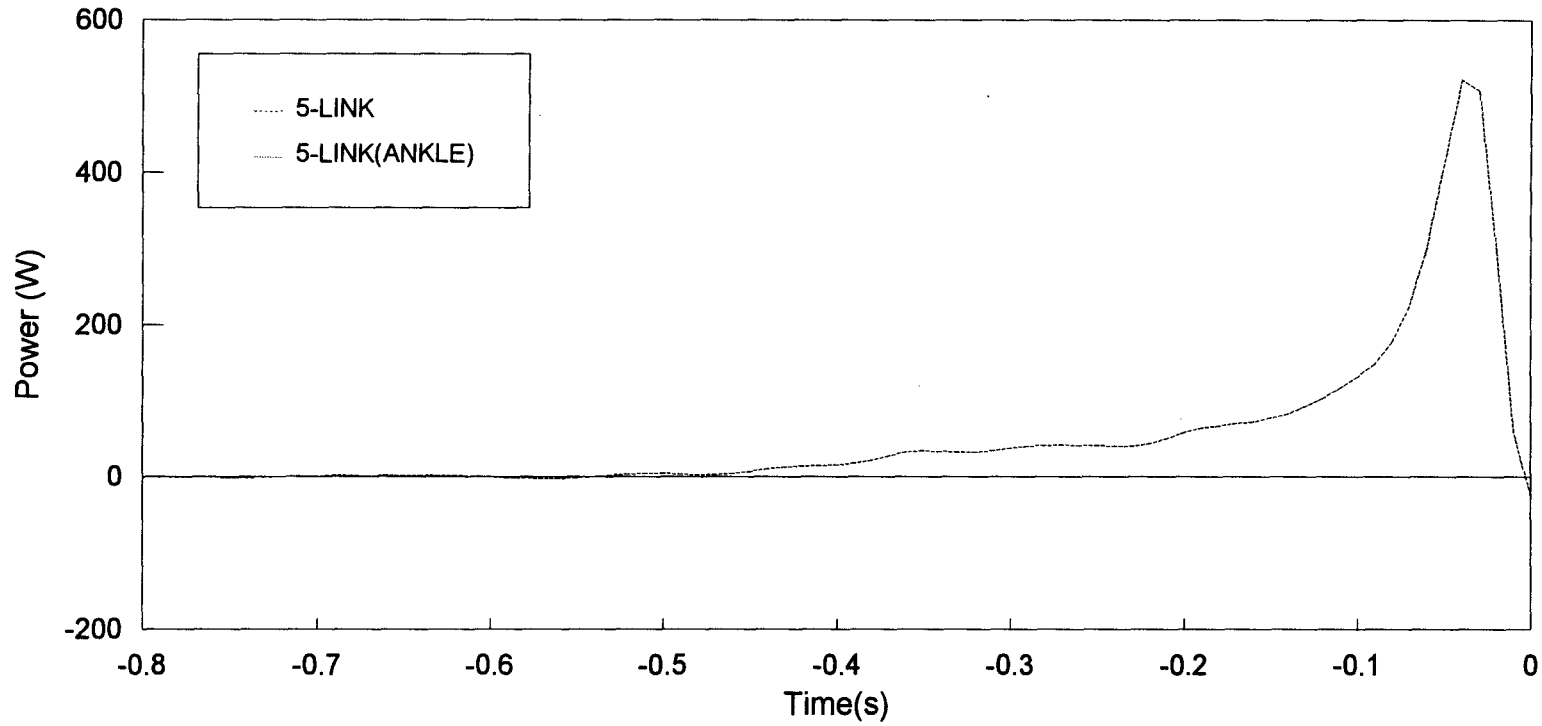


Figure 16. Model Comparison of the Ankle Muscle Power (MP) for a Typical Subject (M1) for a CMJ



**Figure 17.** Model Comparison of the Ankle Moment and the Ankle Angular Velocity for a Typical Subject (M1) for a CMJ

### M-P Joint Power



**Figure 18.** Model Comparison of the M-p Joint Power (JP) for a Typical Subject (M1) for a CMJ

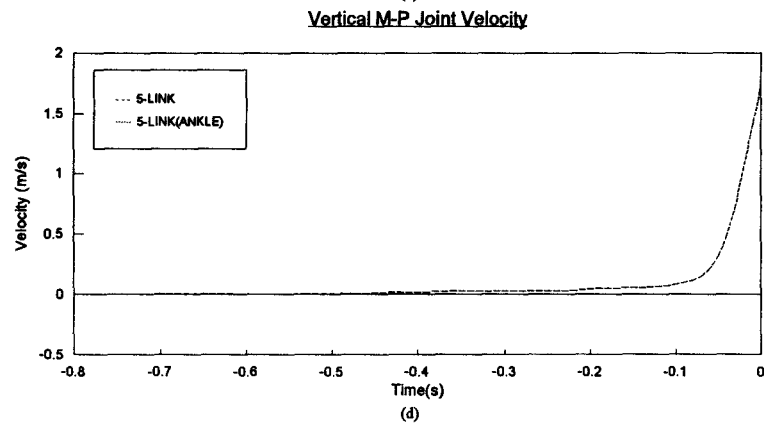
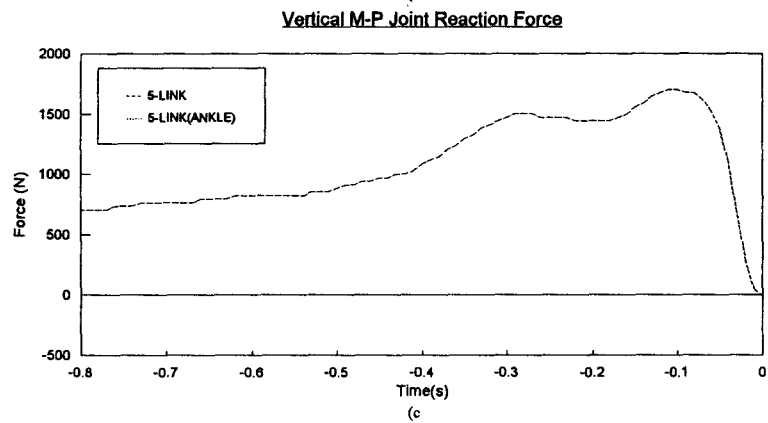
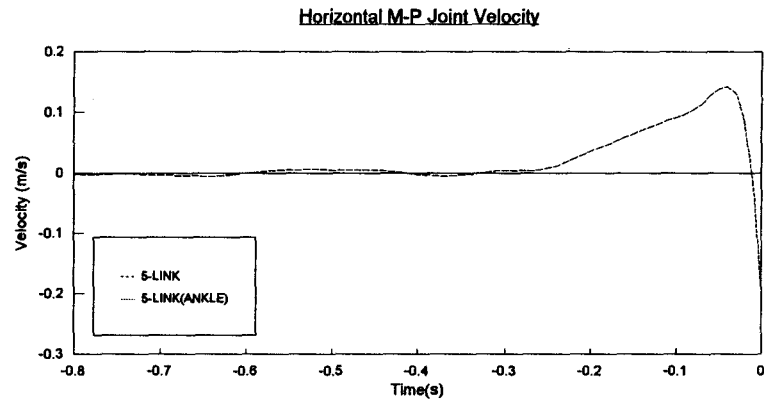
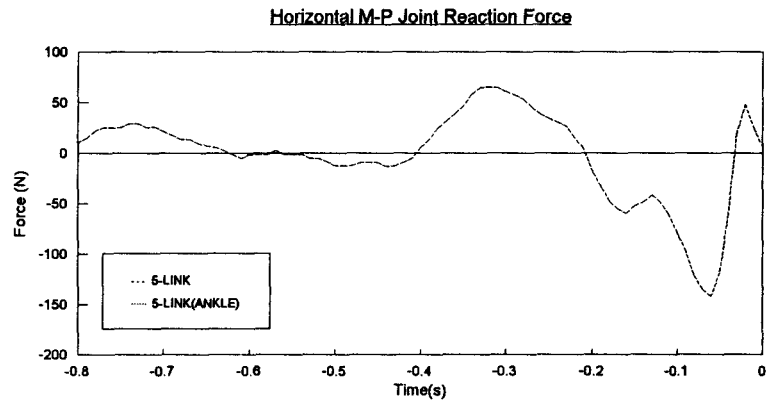


**Figure 19.** Model Comparison of the M-p Joint Reaction Forces and M-p Velocities for a Typical Subject (M1) for a CMJ

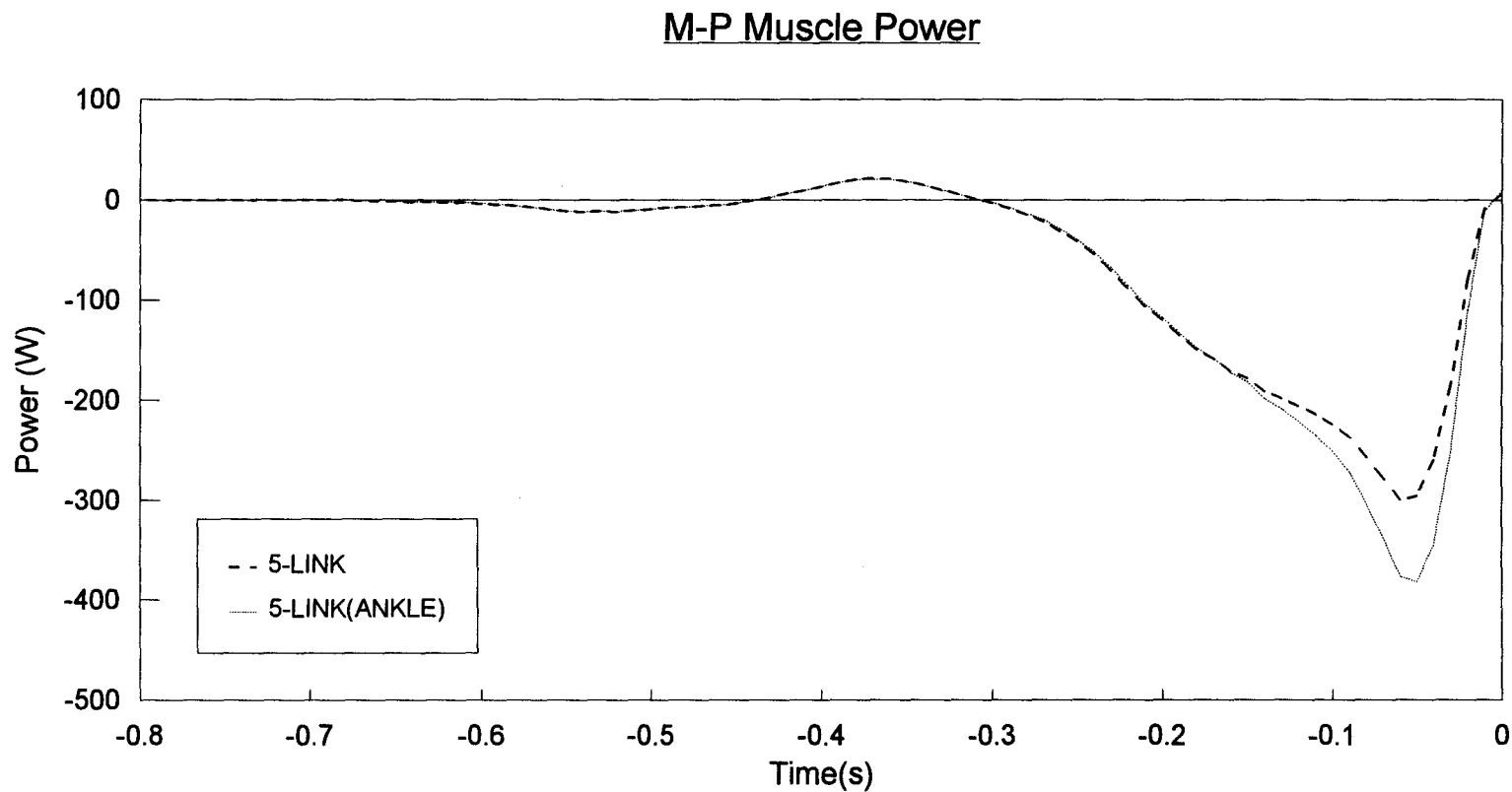


**Figure 20.** Model Comparison of the M-p Muscle Power (MP) for a Typical Subject (M1) for a CMJ

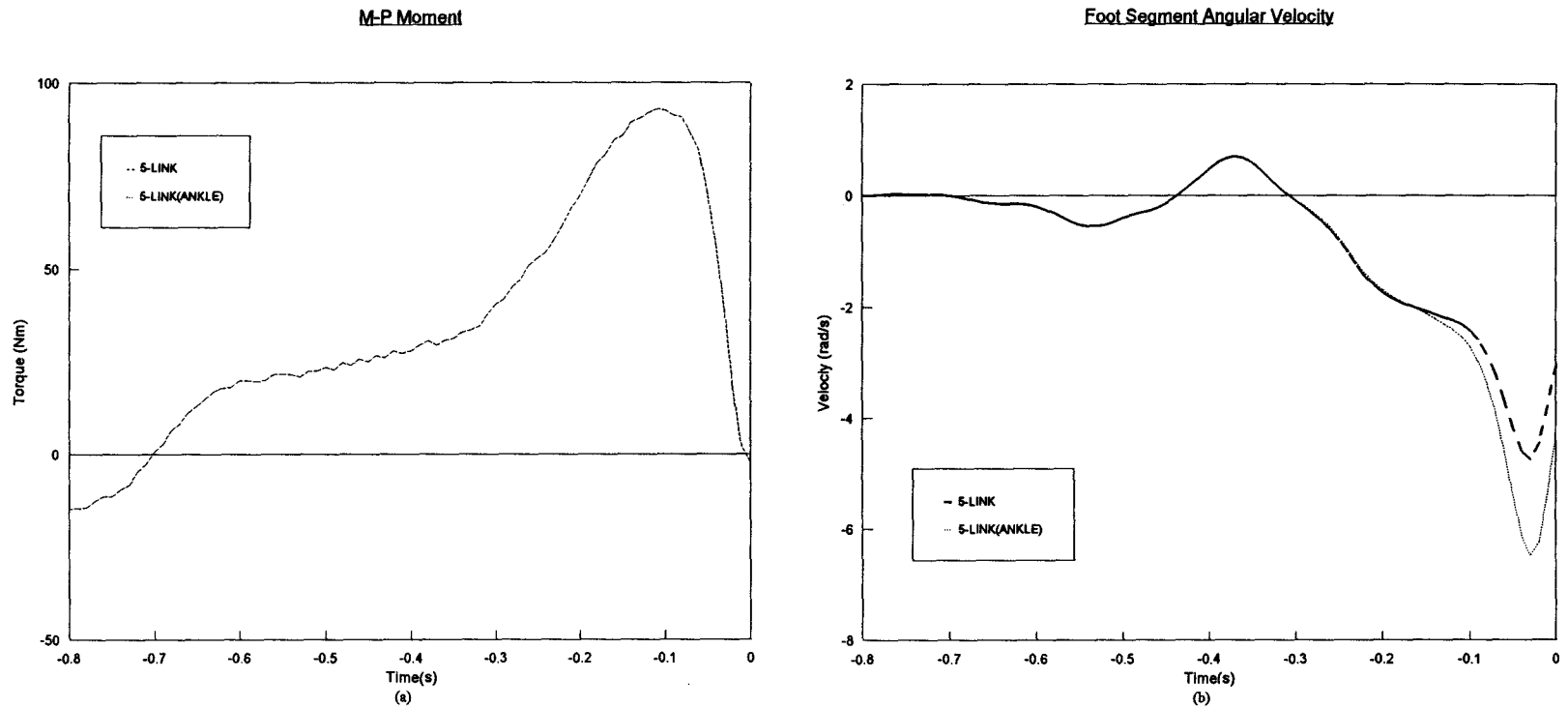


**Figure 21.** Model Comparison of the M-p Moment (a) and the Ankle Angular Velocity (b) for a Typical Subject (M1) for a CMJ

## **Chapter 5**

### **Discussion**

Researchers have used Pearson's product-moment correlations and/or curve comparison to assess differences between the TSP and RCE curves in the absence of inferential statistics. Young and Marteniuk (1995) have reported valid measures based on curve comparison, whereas Robertson and Winter (1980) and Vardaxis and Hoshizaki (1989) have reported valid measures based on Pearson's product-moment correlation coefficients. In this study, both Pearson's correlation coefficients and curve comparison, as well as %RMS error scores, were used to assess the difference between the TSP and RCE. In the literature, the lowest correlation coefficient reported for a segment considered to be valid was 0.815 (Robertson & Winter, 1980). Accordingly, for this study, obtaining Pearson's correlation coefficient of 0.80 or greater, and %RMS error values of less than 60% indicated an acceptable match between TSP and RCE.

#### **5.1 Model Development**

In order to develop a valid foot model for the calculation of TSP in the vertical jump, a combination of both modifications (section 5.1.1 and 5.1.3) to the traditional 4-Link model were necessary. Figures 7b and 7c show that the neither of the modifications on their own resulted in a good match between the TSP and RCE. Tables 14 and 15 show that the 5-Link(ankle) model resulted in substantial improvements for all subjects.

### 5.1.1 Addition of Forefoot Segment

The rationale behind adding a forefoot segment to create the 5-Link model and 5-Link(ankle) model was to include m-p JP and m-p MP at the distal end of the foot segment. The improvement, in the match between the TSP and RCE, with the addition of the forefoot segment indicates that substantial JP and MP occur at the m-p joint in the vertical jump. Figures 13b and 13d illustrate the potential contribution of these powers for a typical subject (M1), at the m-p joint. Associated improvements are noted through a comparison of the curves in Figures 13c and 13d. Here, the negative m-p MP and the positive m-p JP in the 5-Link(ankle) model, compensate for the deflections of the TSP curve for the 4-Link(ankle) model. This compensation will be discussed in more detail in section 5.3.

### 5.1.2 Ankle Location and its Effect on Foot Segment Length

Discrepancies found between the TSP and RCE have been attributed to variations in segment length (van Ingen Schenau & Cavanagh, 1990; de Looze et al, 1992). Causes of segment length changes could be due to true deformation of the segment (i.e. flexion of intermediate joints, non-ideal articulations), to errors in estimating joint centres of rotation, to displacement of markers due to skin movement and/or to measurement error.

Foot segment length changes were observed during the jumping motion for all subjects. Strong correlations between the foot segment length and the ankle angle were found for both the CMJ and SQJ conditions (see Table 9). They indicate a direct

relationship between plantarflexion and increases in foot segment length, and between dorsiflexion and decreases in foot segment length (see Figure 6). This relationship indicated that ankle marker placement may not have been at the true location of the ankle joint. Further, because of the relationship noted between ankle angle and the direction of foot segment length changes, it was determined that the marker placement may have been proximal to the ideal location. Thus for each trial, the ankle joint was relocated by extending the leg segment, such that the segment length changes were reduced to a minimum (see Table 11).

Figure 6a and 6c illustrate substantial improvements to the foot segment rigidity with ankle marker relocation. This new location resulted in a very stable foot segment length (Figure 9), for most subjects. However, some subjects were left with residual segment length changes (Figure 11). These residual length changes may indicate that a different method may be required to find an ideal articulation for the ankle complex for those subjects. Also, other sources of foot segment length variability may have been present. These sources of error could include poor estimation of the m-p joint, skin movement, and translation of the ankle joint centre of rotation during jumping movements.

Two factors could contribute to the an incorrect placement of the ankle marker. Inman (1976) estimated the axis of rotation of the ankle joint to be a line joining two points just distal to each malleolus of the ankle. Accordingly, ankle markers were placed on the most distal end of the bony protuberance of the lateral malleolus of the fibula.

This position was chosen because the IRED markers had to be facing the cameras in order to be detected, and therefore, the most distal part of the fibula was admittedly somewhat lower than the marker placement.

Secondly, findings from Siegler et al. (1988) suggest that the subtalar joint contributes to plantarflexion of the ankle in a non-weight bearing condition. If the subtalar joint contributes to plantarflexion during weight bearing activities such as the vertical jump, the axis of rotation of the ankle complex would be more distal than that originally proposed by Inman (1976). Further investigation of the location of the true centre of rotation of the ankle joint during weight bearing activities is necessary to increase the accuracy and confidence of marker placement.

### 5.1.3. Modification of Ankle Joint Position

Figure 16 shows that the major effect of estimating a better location for a hinge joint to represent the ankle complex, was to increase the ankle MP. Figure 14 shows an accompanying minor increase in the ankle JP. Therefore, with the original ankle position in the 4-Link and 5-Link models, an underestimation of JP and MP may occur. The JP underestimation was due to an underestimation of the horizontal linear velocity of the ankle marker (Figure 15b), while the MP underestimation was due to an underestimation of the ankle muscle moment (up to 30 W) as well as, an underestimation of the foot segment angular velocity (up to 2 rad/s). At peak power, the underestimation of the ankle MP (approx 280 W) was due to a 10% underestimation of the moment and a 20%

underestimation of the angular velocity.

The underestimations for the 4-Link and 5-Link models were greatest when the foot segment appeared to be lengthening, just prior to takeoff. At this point, lengthening of moment arms associated with the joint reaction forces would result in an underestimation of the calculated ankle moment. Also, an apparent lengthening of the foot segment would result in a lower value for the foot segment angular velocity.

## **5.2 Individual Subject Response to Model Modifications**

Trials were divided into three categories based on the correlation coefficients and %RMS error scores (see section 4.3). Trials with final correlations greater than 0.80 were considered as excellent improvements, those with values between 0.5 and 0.80 were considered as good improvements, and correlations less than 0.5 were considered poor improvements. Tables 16 and 17 show that excellent results for the foot segment occurred for the 5-Link(ankle) model in 10 out of the 16 CMJ trials, and 12 out of the 16 SQJ trials. Good results were found for the remaining 6 CMJ trials, and 3 of the 4 remaining SQJ trials. The 5-Link, and 4-Link(ankle) models resulted in poor improvements for the foot segment in all trials.

Subject response in models that included ankle relocation (i.e. 4-Link(ankle), 5-Link(ankle)), was related to the residual segment length changes following ankle relocation (see Figures 9 and 11). The trials in which only good improvements were achieved using the 5-Link(ankle) model were also those trials that had higher values for

the residual segment length variability. Thus, it is suggested that fine tuning of the 5-Link(ankle) model is necessary to achieve excellent improvements for all trials. This may involve further investigation into the ankle centre of rotation or other possible sources of segment length variability (see Section 5.1.2).

### **5.3 Phases of Discrepancy (Comparison with Walking)**

The TSP and RCE curve comparison for the foot segment during a walking trial has been reported to have three phases of discrepancy: a positive deflection of the TSP curve at heel strike, a second positive deflection of the TSP curve at late push-off, which is immediately followed by a third negative deflection of the TSP curve just prior to toe-off (Robertson and Winter, 1980). Winter and Ishac (1994) have postulated that the first discrepancy could be due to energy absorption by the fat pads of the heel at heel strike, the second could be due to energy absorption by the flexing m-p joints, and the third, which immediately follows the second, could be due to energy generation by a push-off from the m-p extensors.

One major phase of discrepancy for the foot segment occurred with the 4-Link and 5-Link models during the vertical jump, just prior to takeoff (Figure 7a and 7b). The negative deflection in the TSP curve was similar to the third phase of the discrepancy for the foot segment in walking reported by Robertson and Winter (1980). However, the magnitude of the discrepancy in the present study, ranged from 4-24 times that reported for walking (Robertson & Winter, 1980).

Two phases of discrepancy were noted for the 4-Link(ankle) model (Figure 7c). An extended positive deflection of the TSP curve followed by a smaller negative deflection was similar to the second and third phases of discrepancy for a walking trial, reported by Robertson and Winter (1980). The magnitude of the negative second deflection was 1-15 times that reported for walking (Robertson & Winter, 1980).

Examination of Figure 13 provides insight into the possible causes of the discrepancies found for the TSP in the vertical jump. Figures 13b and 13d show that the large negative deflection for the TSP curve in the 5-Link model is compensated for when a better estimation of the ankle hinge joint is incorporated (5-Link(ankle) model). Figure 13c and Figure 13d show that the positive deflection of the TSP curve in the 4-Link(ankle) model was compensated for by including the m-p muscle power. Also, the negative deflection of the TSP in the 4-Link(ankle) model was compensated for by adding the m-p joint power to the 4-Link(ankle) model. This suggests that the positive deflection of the TSP curve could be due to the absorption of muscle power at the m-p joint. Also, the negative deflection in the TSP curve could be due to a transfer of joint power from the m-p segment to the foot segment, through the m-p joint.

## **Chapter 6**

### **Conclusions**

This study shows that the addition of a forefoot segment to the traditional foot model, in combination with a modification of the ankle joint location resulted in substantial improvements for the match between the TSP and RCE of the foot segment in the vertical jump. Correlation coefficients between TSP and RCE curves for the foot segment and %RMS error between the two curves, improved substantially for all subjects using the 5-Link(ankle) model. For the CMJ, correlation coefficients improved from -0.46 to 0.92 for the males and from -0.50 to 0.77 for the females, while %RMS error decreased from 380.5% to 35.4% for the males and from 466.9% to 71.6% for the females. For the SQJ, correlation coefficients improved from -0.48 to 0.87 for the males and from -0.45 to 0.79 for the females, while %RMS error decreased from 425.8% to 43.4% for the males and from 417.0% to 59.9% for the females.

Improvements associated with the addition of a forefoot segment to the traditional link-segment model indicate that substantial power flow occurs at the m-p joint for the vertical jump. The inclusion of distal powers at the m-p joint was necessary to achieve acceptable measures of TSP for the foot segment. The use of a forefoot segment in link-segment models used to study other movements, such as walking, will be useful in determining the power flow across the m-p joint in other activities. The net power

contribution of the forefoot segment to the vertical jump was small and occurred very late in the movement.

Success of the ankle relocation in compensating for foot segment length changes indicates that a single point can be located for most subjects, throughout a vertical jump trial, which acts as a hinge joint between the foot and leg segments. This point was located by extending the leg segment, between 1.6cm to 3.2cm for all but one subject. Further investigation is required to identify how this point relates to the true centre of rotation of the ankle complex during weight bearing activities, such as the vertical jump.

The 5-Link(ankle) foot model provided excellent matches between power calculation methods for the majority of skilled jumpers performing either a CMJ or a SQJ. In the present study, correlation coefficients of greater than 0.8 and %RMS error scores of less than 60% were achieved for 10 out of 16 CMJ trials and 12 out of 16 SQJ trials. Application of this model to other weight bearing activities and to different populations is necessary to determine if this model will provide similar improvements throughout. Also, further investigation of those subjects who achieved only good improvements with the 5-Link(ankle) model may give insight to further modifications that could make the model more robust.

Perhaps simply extending the leg segment was not sufficient to locate a better estimation of the ankle joint for some subjects, and more complex methods need to be determined. Also, similar methods used to relocate the ankle joint may be required in estimating the location of the m-p joint. True translations of either of those joints during

a jumping trial, violate the assumptions of traditional link-segment modelling and may require the use of a more sophisticated model. Finally, differences in jumping technique may show that the application of this model is sensitive to certain patterns of movement.

## References

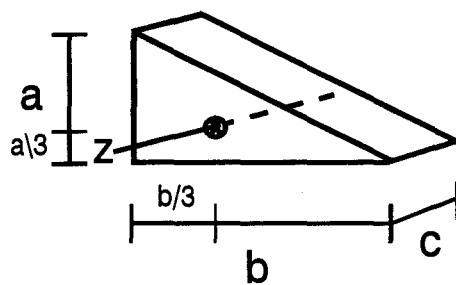
- Caldwell, G. E., and Forrester, L. W. (1992). Estimates of mechanical work and energy transfer: demonstration of a rigid body power model of the recovery leg in gait. Medicine and Science in Sports and Exercise, 24, 1396-1412.
- Chapman, A. E., and Caldwell, G. E. (1983). Factors determining changes in lower limb energy during swing in treadmill running. Journal of Biomechanics, 16, 69-77.
- Clemente, C.D. (Ed.) (1985). Gray's Anatomy (30th American edition). Lea & Febiger, Philadelphia. pp. 408-422.
- Dempster, W. T. (1955). Space requirements of the seated operator (WADC-TR-55-159). Wright-Patterson Air Force Base, Dayton, OH.
- Dowling, J. J., and Vamos, L. (1993). Identification of kinetic and temporal factors related to vertical jump performance. Journal of Applied Biomechanics, 9, 95-110.
- Elftman, H. (1939a). Forces and energy changes in the leg during walking. American Journal of Physiology, 125, 339-356.
- Elftman, H. (1939b). The function of muscles in locomotion. American Journal of Physiology, 125, 357-366.
- Fukashiro, S., and Komi, P. V. (1987). Joint moment and mechanical power flow of the lower limb during vertical jump. International Journal of Sports Medicine, 8 (supplement), 15-21.
- Harman, E. A., Rosenstein, M. T., Frykman, P. N., and Rosenstein, R. M. (1990). The effects of arms and countermovement on vertical jumping. Medicine and Science in Sports and Exercise, 22(6), 825-833.
- Ingen Schenau, G. J. van, and Cavanagh, P. R. (1990). Power equations in endurance sports. Journal of Biomechanics, 23, 865-881.
- Inman, V. T. (1976). The Joints of the Ankle. Williams & Wilkins, Baltimore.

- Lehmkuhl, L. D., and Smith, L. K. (1983). Brunnstrom's Clinical Kinesiology (4th ed.) F.A. Davis, Philadelphia. pp.311-336.
- Looze, M. P. de, Bussmann, J. B. J., Kingma, I., and Toussaint, H. M. (1992). Different methods to estimate total power and its components during lifting. Journal of Biomechanics, 25, 1089-1095.
- Lundberg, A., Nemeth, G., Svensson, O. K., and Selvik, G. (1989). The axis of rotation of the ankle joint. Journal of Bone and Joint Surgery, 71-B, 94-99
- Perrine, J. J., Gregor, R., Munroe, R., and Edgerton, V. R. (1978). Muscle power capacities & temporal output patterns of skilled vs. non-skilled vertical jumpers (abstract). Medicine and Science in Sports and Exercise, 10, 64.
- Plagenhoef, S., Evans, F. G., and Abdelnour, T. (1983). Anatomical data for analyzing human motion. Research Quarterly for Exercise and Sport, 54(2), 169-178.
- Quanbury, A. O., Winter, D. A., and Reimer, G. D. (1975). Instantaneous power and power flow in body segments during walking. Journal of Human Movement Studies, 1, 59-67.
- Robertson, D. G., and Winter, D. A. (1980). Mechanical energy generation, absorption and transfer amongst segments during walking. Journal of Biomechanics, 13, 845-854.
- Sammarco, J. (1977). Biomechanics of the ankle: I. Surface velocity and instant center of rotation in the sagittal plane. American Journal of Sports Medicine, 5(6), 231-234.
- Siegler, S., Chen, J., and Schenck, C.D. (1988). The three-dimensional kinematics and flexibility characteristics of the human ankle and subtalar joint -- Part I: Kinematics. Journal of Biomechanical Engineering, 110, 364-373.
- Vardaxis, V., and Hoshizaki, T. B. (1989). Power patterns of the leg during the recovery phase of the sprinting stride for advanced and intermediate sprinters. International Journal of Sport Biomechanics, 5, 332-349.
- Winter, D. A. (1983). Moments of force and mechanical power in jogging. Journal of Biomechanics, 16, 91-97.

- Winter, D. A. (1990). Biomechanics and Motor Control of Human Movement. (2nd ed.) Wiley & Sons, New York.
- Winter, D. A., and Ishac, M. (1994). Energetics of human locomotion: Modelling and interpretation. In, Proceedings of the Eighth Biennial Conference of the Canadian Society for Biomechanics, (pp. 8-9). Calgary, Alberta.
- Winter, D. A., Quanbury, A. O., and Reimer, G. D. (1976). Instantaneous energy and power flow in gait of normals. In, P.V. Komi (Ed.), Biomechanics V-A (pp. 334-340), University Park Press, Baltimore.
- Young, R. P., and Marteniuk, R. G. (1995). Changes in inter-joint relationships of muscle moments and powers accompanying the acquisition of a multi-articular kicking task. Journal of Biomechanics, 28, 701-713.

**APPENDIX A:**  
**Anthropometric Calculations**

## Right Triangular Prism



$$V = \frac{1}{2}abc$$

$$I_z = \frac{m(a^2 + b^2)}{18}$$

**Figure Used to Calculate Anthropometric Values for the Forefoot Segment**

## Determining the Location of Centre of Gravity for the Hindfoot Segment

The following formula was used to calculate the position of the centre of gravity for the hindfoot in the x-direction,

$$m_F x_{CofG_F} = m_{HF} x_{CofG_{HF}} + m_{FF} x_{CofG_{FF}}$$

$$x_{CofG_{HF}} = \frac{m_F x_{CofG_F} - m_{FF} x_{CofG_{FF}}}{m_{HF}}$$

where,  $m$  is the mass of the segment  
 $x_{CofG}$  is the position of the centre of gravity in the x-direction  
 $F$  denotes the foot  
 $HF$  denotes the hindfoot  
 $FF$  denotes the forefoot

For the female subjects, the position was calculated as follows,

$$x_{CofG_{HF}} = \frac{0.0266(0.5L) - 0.0045(L + 0.28167L)}{0.022}$$

$$x_{CofG_{HF}} = 0.337L$$

For the male subjects, the position was calculated as follows,

$$x_{CofG_{HF}} = \frac{0.0286(0.5L) - 0.0048(L + 0.265L)}{0.0238}$$

$$x_{CofG_{HF}} = 0.346L$$

where,  $L$  denotes the horizontal length of the foot segment

The centre of gravity was only adjusted in the horizontal direction and the proportion was applied to the length between the mp and ankle markers to ensure that the centre of gravity was located on the rigid link joining the two segment endpoints.

## Radius of Gyration for the Hindfoot Segment

Legend: I is the moment of inertia of the segment  
 m is the mass of the segment  
 k is the radius of gyration  
 $d_{X-Y}$  is the distance between x and y  
 $F$  denotes the foot segment  
 $FF$  denotes the forefoot segment  
 $HF$  denotes the hindfoot segment  
 TBM is the total body mass  
 L is the length of the foot segment (mp-ank)

For a composite body, expressed about the same centre of rotation,

$$I_{HF} = I_F - I_{FF}$$

therefore, using parallel axis theorem to express the moments of inertia about the centre of mass of the foot (CofM),

$$(I_{HF} + m_{HF} \cdot d_{HF-CofM}^2) = I_F - (I_{FF} + m_{FF} \cdot d_{FF-CofM}^2)$$

$$(m_{HF} \cdot k_{HF}^2 + m_{HF} \cdot d_{HF-CofM}^2) = m_F \cdot k_F^2 - (m_{FF} \cdot k_{FF}^2 + m_{FF} \cdot d_{FF-CofM}^2)$$

$$k_{HF}^2 = \frac{m_F \cdot k_F^2 - m_{FF} (k_{FF}^2 + d_{FF-CofM}^2)}{m_{HF}} - d_{HF-CofM}^2$$

For the male subjects, the radii of gyration about each segment's centre of gravity ( $k$ ) and the segment masses ( $m$ ) were,

$$k_F = 0.475L$$

$$k_{FF} = 0.252(0.719L) = 0.181L$$

$$m_F = 0.0286TBM$$

$$m_{FF} = 0.0048TBM$$

$$m_{HF} = 0.0238TBM$$

therefore,

$$k_{HF}^2 = \frac{(0.0286TBM)(0.475L)^2 - (0.0048TBM)((0.181L)^2 + (0.740)^2)}{0.0238TBM} - (0.154L)^2$$

$$k_{HF}^2 = 0.1304L^2$$

$$k_{HF} = 0.361L$$

For the female subjects, the radii of gyration about each segment's centre of gravity ( $k$ ) and the segment masses ( $m$ ) were,

$$k_F = 0.475L$$

$$k_{FF} = 0.249(0.755L) = 0.188L$$

$$m_F = 0.0266TBM$$

$$m_{FF} = 0.0045TBM$$

$$m_{HF} = 0.0221TBM$$

therefore,

$$k_{HF}^2 = \frac{(0.0266TBM)(0.475L)^2 - (0.0045TBM)((0.188L)^2 + (0.752)^2)}{0.0221TBM} - (0.163L)^2$$

$$k_{HF}^2 = 0.123L^2$$

$$k_{HF} = 0.350L$$

## Forefoot Anthropometrics

Subject	TBM (kg)	Forefoot Volume (cm <sup>3</sup> )	Forefoot Length (cm)	Forefoot Breadth (cm)	Forefoot Height (cm)	Forefoot Mass (kg)	Forefoot Mass %TBM	Moment of Inertia (kg/cm <sup>2</sup> )	Radius of Gyration/ Seg Length
M1	79.7	155	10.1	9.6	3.2	0.171	0.214	1.06E-04	0.25
M2	93.1	202	9.7	11.7	3.6	0.222	0.239	1.32E-04	0.25
M3	71.8	158	9.6	10.0	3.3	0.174	0.242	9.94E-05	0.25
M4	111.8	225	11.6	11.6	3.3	0.248	0.221	2.00E-04	0.25
M5	86.8	205	9.2	11.2	4.0	0.226	0.260	1.26E-04	0.26
M6	74.2	158	9.1	11.1	3.1	0.174	0.234	8.94E-05	0.25
M7	68.5	163	8.4	10.0	3.9	0.179	0.262	8.53E-05	0.26
M8	83.0	180	9.3	10.3	3.8	0.198	0.239	1.11E-04	0.25
Mean	83.6	180.8	9.6	10.7	3.5	0.199	0.239	1.19E-04	0.25
SD	13.1	25.0	0.9	0.8	0.3	0.028	0.015	3.44E-05	0.00
F1	55.1	140	9.3	8.9	3.4	0.154	0.279	8.38E-05	0.25
F2	66.9	125	8.7	9.0	3.2	0.138	0.206	6.56E-05	0.25
F3	76.3	150	9.4	9.9	3.2	0.165	0.216	9.05E-05	0.25
F4	68.1	140	9.4	9.8	3.0	0.154	0.226	8.35E-05	0.25
F5	70.0	165	9.4	9.4	3.7	0.182	0.259	1.03E-04	0.25
F6	67.4	120	9.0	9.4	2.8	0.132	0.196	6.53E-05	0.25
F7	60.1	100	8.7	9.1	2.5	0.110	0.183	5.02E-05	0.25
F8	71.1	157	9.5	9.6	3.4	0.173	0.243	9.80E-05	0.25
Mean	66.9	137.1	9.2	9.4	3.2	0.151	0.226	8.00E-05	0.25
SD	6.2	19.9	0.3	0.3	0.4	0.022	0.031	1.70E-05	0.00

## Hindfoot Anthropometrics

Subject	TBM (kg)	Footlength mp-heel (cm)	Ffootlength/ mp-heel (ratio)	Foot Lngth mp-ankle (cm)	Ffootlength/ mp-ankle (ratio)	Foot Incln Angle (degrees)
M1	79.7	11.1	13.964	12.5	12.370	36.3
M2	93.1	13.2	15.303	14.3	14.083	34.8
M3	71.8	10.3	15.340	11.2	14.091	34.7
M4	111.8	13.3	16.917	15.0	14.971	36.2
M5	86.8	12.1	16.942	13.3	15.399	35.0
M6	74.2	11.2	14.107	12.4	12.696	35.5
M7	68.5	13.9	11.727	15.3	10.679	35.0
M8	83.0	12.6	14.286	13.9	12.938	35.4
Mean	83.6	12.2	14.823	13.5	13.403	35.4
SD	13.1	1.2	1.601	1.3	1.440	0.5
F1	55.1	10.2	13.725	11.7	11.955	37.1
F2	66.9	10.5	11.905	11.8	10.622	35.9
F3	76.3	10.7	14.019	11.9	12.637	35.6
F4	68.1	10.2	13.725	11.4	12.312	35.7
F5	70.0	10.9	15.138	12.1	13.598	35.6
F6	67.4	12.5	9.600	13.8	8.719	35.1
F7	60.1	10.2	9.804	11.5	8.709	36.2
F8	71.1	12.1	12.975	13.5	11.625	35.7
Mean	66.9	10.9	12.611	12.2	11.272	35.9
SD	6.2	0.8	1.885	0.9	1.675	0.5

 - measured values  
 - calculated values

**APPENDIX B:**

**Individual Subject Values pertaining to  
Modificaton of Ankle Joint Position**

**Correlation coefficients of foot length with ankle angle**

Subject	CMJ Foot	SQJ Foot
M1	0.973	0.995
M2	0.987	0.970
M3	0.989	0.913
M4	0.948	0.984
M5	0.996	0.996
M6	0.909	0.986
M7	0.552	0.908
M8	0.872	0.989
F1	0.794	0.980
F2	0.994	0.995
F3	0.942	0.992
F4	0.732	0.991
F5	0.785	0.678
F6	0.748	1.000
F7	0.966	0.921
F8	0.983	0.988
Mean M	0.903	0.968
SD M	0.139	0.034
Mean F	0.868	0.943
SD F	0.106	0.103

**Ankle Relocation Distance**

Subject	CMJ (cm)	SQJ (cm)
M1	2.7	2.9
M2	2.7	1.9
M3	2.2	1.9
M4	3.2	3.1
M5	2.1	2.2
M6	2.9	2.8
M7	1.8	1.9
M8	2.7	2.0
F1	2.7	2.5
F2	2.4	2.9
F3	2.4	2.7
F4	1.6	1.8
F5	1.9	2.0
F6	5.0	3.2
F7	3.4	3.0
F8	2.7	2.6
Mean M	2.5	2.3
SD M	0.4	0.5
Mean F	2.8	2.6
SD F	1.0	0.5

Segment Length Variability

Range/Mean\*100%

Subject	CMJ						SQJ					
	Forefoot	Foot (OA)	Foot (RA)	Leg	Thigh	HAT	Forefoot	Foot (OA)	Foot (RA)	Leg	Thigh	HAT
M1	17.6	26.6	3.8	4.4	10.1	15.8	9.8	25.1	3.0	3.7	11.1	19.4
M2	8.1	18.2	2.2	6.7	14.0	20.9	6.5	11.0	1.8	4.3	9.5	10.6
M3	11.2	24.7	4.3	6.6	8.9	13.3	3.0	17.0	4.0	5.7	7.6	13.5
M4	21.2	20.6	5.2	6.0	10.3	25.6	25.8	20.7	2.8	2.3	6.1	21.7
M5	8.9	16.3	1.2	4.6	9.7	26.9	4.1	15.7	1.1	3.2	10.1	25.5
M6	13.0	24.1	8.9	8.6	12.0	21.9	12.3	30.5	5.3	9.3	13.6	13.9
M7	13.0	19.4	9.3	5.5	6.7	24.9	6.2	17.3	5.3	4.5	5.6	17.9
M8	8.1	21.2	7.7	6.5	9.9	22.1	7.0	15.3	2.1	5.9	8.6	15.6
F1	11.9	19.1	7.3	4.6	7.4	23.5	8.4	20.6	3.6	3.9	10.3	20.6
F2	21.7	20.1	1.6	3.7	8.8	18.6	14.7	23.8	2.2	3.4	12.2	15.9
F3	11.3	21.8	4.9	7.0	12.0	15.6	10.9	25.3	2.7	6.6	6.7	15.1
F4	33.3	16.2	8.1	6.9	6.7	14.7	20.3	20.5	3.6	6.4	8.0	19.8
F5	6.3	16.2	4.8	5.4	8.6	16.0	9.5	20.0	9.1	4.2	7.5	20.5
F6	16.0	33.2	20.9	10.4	16.7	19.2	4.6	23.7	0.8	8.4	16.5	12.1
F7	8.7	29.6	4.8	12.1	14.3	27.1	10.9	24.5	6.6	9.2	12.3	23.0
F8	16.9	23.1	3.4	6.5	21.2	23.6	9.8	24.0	3.2	4.7	16.2	20.6
Mean M	12.6	21.4	5.3	6.1	10.2	21.4	9.3	19.1	3.2	4.9	9.0	17.3
SD M	4.4	3.3	2.8	1.3	2.0	4.4	6.8	5.8	1.5	2.0	2.5	4.5
Mean F	15.8	22.4	7.0	7.1	12.0	19.8	11.1	22.8	4.0	5.9	11.2	18.5
SD F	8.0	5.7	5.6	2.7	4.8	4.2	4.4	1.9	2.5	2.0	3.5	3.4

(OA) - original ankle position  
 (RA) - relocated ankle position